NATIONAL ADVISORY COMMITTEE FOR AERONAUTICS

TECHNICAL NOTE 2860

INTERACTION BETWEEN A SUPERSONIC STREAM AND A PARALLEL SUBSONIC STREAM BOUNDED BY FLUID AT REST

By Herbert S. Ribner and E. Leonard Arnoff

Lewis Flight Propulsion Laboratory
Cleveland, Ohio

Washington
December 1952

NATIONAL ADVISORY COMMITTEE FOR AERONAUTICS

TECHNICAL NOTE 2860

INTERACTION BETWEEN A SUPERSONIC STREAM AND A PARALLEL SUBSONIC STREAM BOUNDED BY FLUID AT REST

By Herbert S. Ribner and E. Leonard Arnoff

SUMMARY

In a simplified inviscid model of shock-wave boundary-layer interaction, Tsien and Finston have replaced the boundary layer by a uniform subsonic stream bounded on one side by a solid wall and on the other side by the interface with a uniform supersonic stream of semi-infinite extent. Among other things, this model fails to simulate the separated region or "dead-air" bubble that generally appears in a laminar boundary layer subjected to an oblique incident shock wave of moderate strength. In order to introduce a main feature of such a dead-air region, the model has been modified herein by replacing the solid wall by an interface with fluid at rest.

The presence of the boundary layer sandwiched between the outer supersonic flow and the dead-air region is found scarcely to modify the shape, in the vicinity of the shock, of the expansive "corner" turn that would exist if the shock were incident directly on the dead-air region without the intermediary of the boundary layer; there are local distortions top and bottom, but these are reduced to negligible amounts several boundary-layer thicknesses to the left or right of the effective corner.

In support of a phase of the work of Lester Lees, it is concluded that in a more accurate treatment of the complete region of shock boundary-layer interaction the Prandtl boundary-layer equations may be applied to the entire extent of the disturbed boundary layer, applying as a boundary condition a sudden turn of the displacement surface through twice the shock deflection angle at the point of shock incidence. Thereby the flow details in the immediate vicinity of the shock will be somewhat in error, but the over-all features of the interaction are capable of being given correctly. Present unknown elements in such an application appear to be the point of transition from laminar to turbulent flow and the form of the turbulent equations where a separated bubble exists.

INTRODUCTION

The complex problem of the interaction between shock waves and boundary layers in supersonic flow is not yet clearly understood, despite a number of theoretical studies (references 1 to 7). Among these, the analysis of Tsien and Finston (reference 2) is singled out here for further examination. In the Tsien-Finston model the boundary layer is simulated by a uniform subsonic stream of finite width bounded on one side by a solid wall and on the other side by the interface with a uniform supersonic stream of semi-infinite extent. The fluid is assumed to be nonviscous and nonheat-conducting and the disturbances are assumed small.

The boundary-layer perturbation calculated in reference 2 from this model has the general character shown in sketch 1. The experimental perturbation for a laminar boundary layer (e.g., references 8 and 9), on the other hand, has the general character shown in sketch 2. The resemblance is not close. A striking experimental feature is the presence of a separated region, which appears for all but the weakest incident shock strengths (references 3 and 9). The separated region is not simulated in the Tsien-Finston model of shock boundary-layer interaction, and this constitutes an important shortcoming of the model for laminar boundary layers. For turbulent boundary layers subjected to moderate shock strengths, on the other hand, there will be no separation, and the model may be quite good.

The air in a separated bubble is substantially at rest. An oblique shock incident directly on a dead-air region, without the intermediary of a boundary layer, is known to reflect as an expansion wave (see sketch 3). Note that the interface in sketch 3 is deflected much like the potential flow just above the actual boundary layer (sketch 2), a feature completely unduplicated in the Tsien-Finston model (sketch 1). A natural inference is that the separated region dominates the behavior in the immediate vicinity of the shock, and the upper surface behaves, in that vicinity, substantially as if the entire boundary layer were replaced by a dead-air region.

This tempting inference has been made to provide a boundary condition in the work of Lees (reference 6) and of Ritter (reference 7), along with other simplifying assumptions; it is the purpose of the present paper to test its validity on a simplified model applicable only to the immediate vicinity of the shock. For this purpose a modification of the Tsien-Finston model will serve: the solid lower wall of sketch 1 is replaced by a semi-infinite region of air at rest, or "dead air". Thus the boundary condition of zero vertical perturbation velocity at the wall is replaced by a condition of constant pressure along the boundary of the dead-air region; in all other respects there is no change from the original model. Experimentally (reference 9), an approximation to

the condition of constant pressure is found over a substantial portion of the separated air bubble including the part directly under the incident shock; the ultimate sharp pressure rise generally occurs somewhat downstream of the shock.

It has been implicit in the discussion that attention was limited to the boundary layer adjacent to a solid body. Also of interest, however, is the boundary layer between a two-dimensional supersonic jet and the stationary fluid bounding it. The present modified flow model will describe, in idealized fashion, the interaction of an oblique shock wave (such as may emanate from a nozzle lip) with such a jet boundary layer. The model is, in fact, better adapted to such a fluid-to-fluid boundary layer than it is to the fluid-to-wall boundary layer.

The mathematical analysis herein of the modified model is necessarily parallel in a number of respects to the original work of Tsien and Finston. Nevertheless, it has been thought worthwhile to provide a complete account in an appendix for purposes of unity and clarity. The symbols used in this analysis are presented in appendix A; the analysis, in appendix B. An abbreviated version of the analysis is given in the main text. The investigation was conducted at the NACA Lewis laboratory.

SYNOPSIS OF ANALYSIS

Flow regions and governing equations. - In figure 1 are shown the supersonic region (region 1) at the top, the subsonic region (region 2) in the middle, and the dead-air region (region 3) at the bottom. A weak shock wave, or Mach wave, is incident on the interface between regions 1 and 2. The governing equations for the perturbation potential are

$$\text{Region 1:} \quad \left(1 - M_1^2\right) \frac{\partial^2 \varphi_1}{\partial x^2} + \frac{\partial^2 \varphi_1}{\partial y^2} = 0, \quad M_1 > 1$$

$$\text{Region 2:} \quad \left(1 - M_2^2\right) \frac{\partial^2 \varphi_2}{\partial x^2} + \frac{\partial^2 \varphi_2}{\partial y^2} = 0, \quad M_2 < 1$$

In region 1 the perturbation potential includes a part (incoming wave) which represents directly the incident Mach wave and a part (outgoing waves) which arises from the consequent warping of the interface between regions 1 and 2.

Boundary conditions at each interface. - The boundary conditions are: (a) The perturbation pressure must be the same on both sides of an interface (taken to be zero at the lower interface), and (b) the flow inclination must be the same on both sides. In linearized theory, boundary condition (a) is essentially a condition on the axial perturbation velocity

u, and boundary condition (b) is essentially a condition on the transverse perturbation velocity v. At the lower interface, condition (b) yields no information, since no direction can be assigned to the zero velocity in the bottom region; thus (a) and (b), as applied to both interfaces, yield three boundary conditions.

Solution in general form. - The general solution for each region is expressed in the form of a Fourier integral; such a form is capable of satisfying arbitrary boundary conditions. The variable of integration is λ, and terms like $A_1(\lambda) \cos \lambda x$, $B_1(\lambda) \sin \lambda x$, and so forth, appear; there are six Fourier coefficients $A_1(\lambda)$, $B_1(\lambda)$, $E_2(\lambda)$, $F_2(\lambda)$, $G_2(\lambda)$, and $H_2(\lambda)$ to be determined.

Application of boundary conditions. - The velocity components in Fourier integral form are now substituted into the three boundary conditions; equating corresponding coefficients of sine terms and cosine terms results, in effect, in six equations. Two of the equations yield $E_2(\lambda) = F_2(\lambda) = 0$; thus there remain four equations which are solved simultaneously for the four remaining Fourier coefficients $A_1(\lambda)$, $B_1(\lambda)$, $G_2(\lambda)$, and $H_2(\lambda)$.

Solution for pressure along upper interface. - The perturbation pressure along the upper interface is proportional to u_2 there; the expression is of the form of a Fourier integral involving $G_2(\lambda)$ and $H_2(\lambda)$, which are now known. Evaluation and simplification of the integral is complicated and tedious; the final result is expressed in series form and evaluated numerically. In this evaluation, functions tabulated by Tsien and Finston are employed.

Solution for displacement of each interface. - The local displacement $\eta(x)$ of an interface from its undisturbed position is obtained by integration of the slope $d\eta/dx$; this slope is related to v_2 by

$$\frac{d\eta}{dx} \cong \frac{v_2}{U_2}$$

Like u_2, v_2 has been obtained as a Fourier integral involving $G_2(\lambda)$ and $H_2(\lambda)$, and G_2 and H_2 are now known. Again, evaluation and simplification of the integrals is an involved process, and the final displacements are exhibited in series form and evaluated numerically.

RESULTS AND DISCUSSION

Present Modified Tsien-Finston Model

Mach number parameter θ. - In the results herein the Mach numbers M_1 and M_2 of the respective supersonic and subsonic streams appear in

a joint parameter θ as well as individually.. For a given value of θ, M_2 is a prescribed function of M_1 (see equation (B32)). The curves of M_2 against M_1 for several values of θ are given in figure 2, which has been reproduced from figure 3 of reference 2. Tsien and Finston note that if the representative Mach numbers for the boundary-layer flow and the free stream are taken to be 0.8 and 2, respectively, then the corresponding value of θ in the flow model is approximately $3\pi/4$.

Pressure distribution. - Curves of the pressure distribution along the upper interface calculated from equations (B62) and (B63) with the aid of functions tabulated in reference 2 are given in figures 3(a), 3(b), and 3(c) for values $\pi/4$, $\pi/2$, and $3\pi/4$, respectively, for the Mach number parameter θ. These curves exhibit the same infinite pressure peak at the point of shock incidence ($\xi = 0$) found by Tsien and Finston with the original model. A similar peak was found by Lighthill (reference 5) in his model with continuous, rather than stepwise, velocity profile; in that case the peak occurred inside the simulated boundary layer at the point of reflection of the shock from the sonic line. Such a peak will be modified in a real flow and probably will appear as a localized region of high pressure.

Displacement of upper and lower interfaces. - The respective displacements of the upper and lower interfaces from their undisturbed positions have been designated η_U and η_L; both are functions of the longitudinal distance x. Convenient corresponding nondimensional parameters are $\frac{\pi}{2b\beta_2}\frac{\eta_U}{2\epsilon}$, $\frac{\pi}{2b\beta_2}\frac{\eta_L}{2\epsilon}$, and $\frac{\pi x}{2b\beta_2}$. Curves of the displacement against longitudinal distance in terms of these nondimensional parameters are plotted in figures 4(a), 4(b), and 4(c) for θ equal to $\pi/4$, $\pi/2$, and $3\pi/4$, respectively. The infinite slope at $x = 0$, associated with the pressure peak there, is so localized on the drawings as to be scarcely distinguishable.

The scales are such that the vertical and horizontal displacements of a given interface are to the same geometric scale for the case $\epsilon = 1/8$ radian; for this value of ϵ the separation of the interfaces is to correct scale when, in addition, $\beta_2 = \pi/20$ for $\theta = \pi/4$ ($M_1 = 2.5$, $M_2 = 0.988$); $\beta_2 = \pi/10$ for $\theta = \pi/2$ ($M_1 = 2.7$, $M_2 = 0.95$); and $\beta_2 = \pi/6$ for $\theta = 3\pi/4$ ($M_1 = 3.1$, $M_2 = 0.85$). Numerical values of the ordinates and abscissas are also tabulated in tables I and II.

Comparison with supersonic flow above still air, no boundary layer. - The curves are now to be compared with the conjecture given in the introduction: namely, that in the simplified model of figure 1 the upper interface behaves, in the vicinity of the shock, substantially as if the entire boundary layer (represented by region 2) were replaced by a dead-air region (an extension of region 3); that is, that the upper interface

deflects through an angle 2ε just as the dead-air interface does in sketch 3. The comparison shows that the curves in figure 4 approximate the conjectured behavior; both interfaces asymptotically approach the expansive turn through an angle 2ε.

For each interface, the final asymptote does not intersect the initial asymptote (which is the ξ-axis) at the point of shock incidence, $\xi = 0$; instead the point of intersection lies somewhat downstream thereof. The point of intersection of the two asymptotes may be thought of as the effective "corner" for the turn through 2ε; its displacement amounts from one to several "reduced" boundary-layer thicknesses (reduced thickness = $b\beta_2$), depending on the value of the Mach number parameter θ. The local deviation from the asymptotic behavior, that is, from the rectilinear corner turn of sketch 3, is limited essentially to several reduced boundary-layer thicknesses upstream and downstream of the effective corner.

Further Generalization of Tsien-Finston Model and Limitations

The flow model of figure 1 is supposed to simulate only one aspect of shock boundary-layer interaction, namely, the local effect of the separated region in the vicinity of the point of shock incidence. An obvious further generalization, later found to be of questionable utility, is sketched in figure 5. Here the dead-air region is limited to a finite length to approximate the "separation bubble," and on either side thereof the solid-wall condition used by Tsien and Finston is reapplied.

When points S and R are both more than several reduced boundary-layer thicknesses from I, the point of shock incidence, their effects in the neighborhood of I would be expected to be small. This consideration serves to justify the use, for the neighborhood of I, of the model of figure 1 in which S and R are effectively removed to minus and plus infinity, respectively.

There is another mentionable difference between the models of figures 1 and 5: In figure 1 the perturbation pressure in the dead-air region is taken to be zero (for simplicity), whereas a positive perturbation pressure is intended in figure 5. The pressure rise in figure 5 is effected by means of a weak shock or Mach wave incident just above S, resulting in the general upward slope of the boundary layer between S and I. This more realistic positive pressure perturbation in the dead-air region may be introduced into the model of figure 1 by imagining the weak shock associated with point S to occur at minus infinity to the left. Then the entire flow field will have an upward deflection (say ε_1) corresponding to the flow deflection through this shock. As a consequence, the interface deflections of figure 4 will have superposed a

deflection $\eta = \varepsilon_1 x$ (or $\frac{\pi}{2\pi\beta_2}\frac{\eta}{2\varepsilon} = \frac{\pi x}{2\pi\beta_2}\cdot\frac{\varepsilon_1}{2\varepsilon}$); this is substantially as though each figure were rotated counterclockwise through the angle ε_1.

As a generalization from a single aspect to a more complete picture of shock boundary-layer interaction, the model of figure 5 has serious shortcomings. The model by itself is insufficient to determine the positions of separation and reattachment S and R; for this purpose the neglected viscosity will have to be brought into the picture. Moreover, between I and R the actual boundary-layer flow will probably become turbulent, and the neglected turbulent momentum exchange across both of the idealized interfaces will markedly influence the shape of the effective interfaces and the location of R. The transition to turbulent flow will probably be decisive in determining R unless the incident shock is relatively weak, since otherwise the large abrupt pressure rise upon reattachment would be expected to reseparate a laminar layer but not a turbulent one. For these reasons it has not seemed worthwhile to make a serious effort to obtain an analytical solution for this model.

Applicability of the Assumptions of Boundary-Layer Theory

On the present model of shock boundary-layer interaction, the region in which the upper and lower interfaces show substantial curvatures and deviations from parallelism has been shown to be limited to one or two reduced boundary-layer thicknesses on either side of the point of shock incidence; a similar result is found for the original Tsien-Finston model. These results imply that it is only in this region that the component pressure gradient dp/dy is significant. Elsewhere the primary assumption of the Prandtl boundary-layer theory, namely, that dp/dy may be neglected, appears to be applicable.

The situation seems to be as follows: Both models of shock boundary-layer interaction completely neglect viscosity, but include the inertial effects in both x- and y-directions, although in idealized fashion. The boundary-layer theory, on the other hand, includes viscosity and the inertia effects in the x-direction alone, the latter with idealization. The results of these models, despite their neglect of viscosity and other idealizations, suffice to delimit the small region directly under the incident shock in which the inertia effects in the y-direction must be included. It appears to be a proper inference that the Prandtl boundary-layer equations, laminar or turbulent as the case may be, and with provision for interaction with the outer flow, may be applied upstream and downstream of this region, except possibly at the point of reattachment of the separated bubble. The separated bubble itself, except that portion directly under the shock, is included in the region of applicability.

Furthermore, the extension of the boundary-layer equations into the forbidden region, with the assumption of a sudden turn of the displacement surface through an angle 2ε at the shock, appears to be justified in a practical analysis where accuracy in local flow details at the shock is secondary to the over-all picture; this conclusion is in support of a phase of the treatments of references 6 and 7. (If the incident shock is too weak to cause a separated bubble, the 2ε turn at the shock must be replaced by another condition.) Present unknown elements in such an application appear to be the choice of the point of transition to turbulent flow, if the boundary layer is not initially turbulent, and equations relating pressure distribution and displacement thickness for a separated region of a turbulent or transitional boundary layer.

Lewis Flight Propulsion Laboratory
National Advisory Committee for Aeronautics
Cleveland, Ohio, September 19, 1952.

[Note added in proof: In a newly published paper ("A Mixing Theory for the Interaction Between Dissipative Flows and Nearly Isentropic Streams," Jour. Aero. Sci., vol. 19, no. 10, Oct. 1952, pp. 649-676) Crocco and Lees have, in effect, supplied the missing relation between pressure distribution and displacement thickness for a turbulent or transitional boundary layer by means of an assumption on the rate of mixing with the outer flow. In their work the boundary layer is replaced by a quasi-one-dimensional flow with the aid of quantities calculated by the Prandtl boundary-layer theory. There is no conflict between the affirmative conclusions of the present paper on the applicability of the Prandtl theory and the position taken in the Crocco-Lees paper.]

APPENDIX A

SYMBOLS

The following symbols are used in this report:

$A_1(\lambda)$, $B_1(\lambda)$	Fourier coefficients appearing in the solutions for the supersonic stream
$E_2(\lambda)$, $F_2(\lambda)$, $G_2(\lambda)$, $H_2(\lambda)$	Fourier coefficients appearing in the solutions for the subsonic stream
$I_1, I_2, \ldots, I_9$	Designation for nine integrals considered in the analysis
b	thickness of subsonic region
f	function of x and y representing incoming waves
g	function of x and y representing outgoing waves
M	Mach number
p	static pressure
Δp	change in static pressure
R	reattachment point in figure 5
$S =$	$2b\lambda\beta_2$; also separation point in figure 5
U	undisturbed velocity
u,v	disturbance velocity components in x- and y-directions, respectively
$w =$	$x + \beta_1 y$
x,y	rectangular Cartesian coordinates
$z =$	λ/γ
$\beta_1 =$	$\sqrt{M_1^2 - 1}$
$\beta_2 =$	$\sqrt{1 - M_2^2}$
γ	parameter introduced in equation (B3)

ε deflection angle of compression wave

η displacement of interface from undisturbed position

θ Mach number parameter defined by $\cos\frac{\theta}{2} = \dfrac{\frac{M_2^2}{M_1^2}}{\sqrt{\left(\frac{M_2^2}{M_1^2}\right)^2 + \frac{\beta_2^2}{\beta_1^2}}}$

λ variable of integration

$\xi =$ $\pi x/2b\beta_2$

$1(\xi)$ step function defined by $1(\xi) \equiv \begin{cases} 0, & \xi < 0 \\ \frac{1}{2}, & \xi = 0 \\ 1, & \xi > 0 \end{cases}$

ρ density

φ disturbance velocity potential

Subscripts:

L value of given function evaluated at the lower interface, $y = -b$

U value of given function evaluated at the upper interface, $y = 0$

$y = +0$ limiting value of given function as y approaches zero through values greater than zero

$y = -0$ limiting value of given function as y approaches zero through values less than zero

1 denotes quantities in the supersonic region $y > 0$ (excepting I_1)

2 denotes quantities in the subsonic region $-b < y < 0$ (excepting I_2)

Superscripts:

* indicates limit of given function as $\gamma \to 0$; for example, $f(\gamma)^* \equiv \lim_{\gamma \to 0} f(\gamma)$

APPENDIX B

ANALYSIS

In the present report, the boundary layer has been replaced by a uniform subsonic stream of finite width b which is bounded on one side by fluid at rest and on the other side by a uniform supersonic stream of semi-infinite extent. For purposes of analysis, this configuration will be considered oriented with respect to a rectangular Cartesian coordinate system such that the positive x-axis is parallel to, and in the direction of, the undisturbed flow and coincides with the undisturbed interface between the subsonic and supersonic streams, and such that the origin denotes the point of incidence of the given shock wave with this interface (see fig. 1). Thus, for $-b < y < 0$ the flow is subsonic, while for $y > 0$ the flow is supersonic. Furthermore, all quantities in the supersonic region will be denoted by the subscript 1 and all quantities in the subsonic region will be denoted by the subscript 2.

Supersonic Region

Governing equation and solution for incoming waves. - In the supersonic stream, the linearized differential equation for the disturbance velocity potential φ_1 is given by

$$\beta_1^2 \frac{\partial^2 \varphi_1}{\partial x^2} - \frac{\partial^2 \varphi_1}{\partial y^2} = 0 \tag{B1}$$

and has as its solution

$$\varphi_1 = f(x + \beta_1 y) + g(x - \beta_1 y) \tag{B2}$$

where f and g are arbitrary functions. The undisturbed flow has been taken in the positive x-direction so that waves represented by $f(x + \beta_1 y)$ will be incoming waves while those represented by $g(x - \beta_1 y)$ will be outgoing waves emanating from the upper interface.

For purposes of the analysis, the form of the function f will be specialized and taken to be

$$f(x + \beta_1 y) = \begin{cases} 0, & x + \beta_1 y < 0 \\ \dfrac{U_1 \varepsilon}{\gamma \beta_1} \left[e^{-\gamma (x + \beta_1 y)} - 1 \right], & x + \beta_1 y > 0 \end{cases} \tag{B3}$$

where U_1 is the undisturbed velocity in the supersonic stream and where γ and ε are parameters. If γ tends to zero, the incoming waves will degenerate into a single compression wave with deflection

angle ε, and the point of incidence of this single compressive wave with the upper interface will be the origin of the given rectangular Cartesian coordinate system.

Now, by definition, the components u and v of the disturbance velocity are given in terms of the disturbance velocity potential φ by the relations

$$u = \frac{\partial \varphi}{\partial x}; \quad v = \frac{\partial \varphi}{\partial y} \tag{B4}$$

Therefore, the components of the disturbance velocity of the incoming waves are given by

$$u_{1,\text{incoming}} = \begin{cases} 0 & , \quad x + \beta_1 y < 0 \\ \dfrac{-U_1 \varepsilon}{\beta_1} e^{-\gamma(x + \beta_1 y)}, & x + \beta_1 y > 0 \end{cases} \tag{B5}$$

and

$$v_{1,\text{incoming}} = \begin{cases} 0 & , \quad x + \beta_1 y < 0 \\ -U_1 \varepsilon e^{-\gamma(x + \beta_1 y)}, & x + \beta_1 y > 0 \end{cases} \tag{B6}$$

Incoming and outgoing waves in Fourier-integral form. - It will prove useful to express the disturbance velocities of the incoming waves in the equivalent Fourier-integral form. To do this, it is noted that the components of the disturbance velocity of the incoming waves are proportional to the function

$$h(w) \equiv \begin{cases} 0 & , \quad w < 0 \\ e^{-\gamma w}, & w > 0 \end{cases} \tag{B7}$$

where $w \equiv x + \beta_1 y$, and that $h(w)$ can be represented in an entirely equivalent form by

$$h(w) = \frac{1}{\pi} \int_C \left(\frac{\gamma}{\gamma^2 + \lambda^2} \cos \lambda w + \frac{\lambda}{\gamma^2 + \lambda^2} \sin \lambda w \right) d\lambda \tag{B8}$$

Furthermore, the potential due to the outgoing waves can also be expressed in Fourier-integral form, namely,

$$g(x - \beta_1 y) = U_1 \int_0^{\infty} \left[A_1(\lambda) \sin \lambda(x - \beta_1 y) + B_1(\lambda) \cos \lambda(x - \beta_1 y) \right] d\lambda \tag{B9}$$

where $A_1(\lambda)$ and $B_1(\lambda)$ are undetermined Fourier coefficients. Thus, after differentiation of the expression for $g(x - \beta_1 y)$ to obtain the disturbance velocities due to the outgoing waves, the separate disturbance velocities can be superposed and the Fourier-integral expressions for the components of the total disturbance velocities (of both incoming and outgoing waves) obtained. Evaluated at the upper interface, these disturbance velocity components will then be given by

$$u_{1,y=+0} = \frac{-\varepsilon U_1}{\pi \beta_1} \int_0^{\infty} \left(\frac{\gamma}{\gamma^2 + \lambda^2} \cos \lambda x + \frac{\lambda}{\gamma^2 + \lambda^2} \sin \lambda x \right) d\lambda + U_1 \int_0^{\infty} \left[\lambda A_1(\lambda) \cos \lambda x - \lambda B_1(\lambda) \sin \lambda x \right] d\lambda \tag{B10}$$

and

$$v_{1,y=+0} = \frac{-\varepsilon U_1}{\pi} \int_0^{\infty} \left(\frac{\gamma}{\gamma^2 + \lambda^2} \cos \lambda x + \frac{\lambda}{\gamma^2 + \lambda^2} \sin \lambda x \right) d\lambda - \beta_1 U_1 \int_0^{\infty} \left[\lambda A_1(\lambda) \cos \lambda x - \lambda B_1(\lambda) \sin \lambda x \right] d\lambda \tag{B11}$$

Subsonic Region

Governing equation and general solution in Fourier-integral form. - For the subsonic stream, $-b < y < 0$, the linearized differential equation for the disturbance velocity potential is given by

$$\beta_2^2 \frac{\partial^2 \Phi_2}{\partial x^2} + \frac{\partial^2 \Phi_2}{\partial y^2} = 0 \tag{B12}$$

and the solution φ_2 can be expressed, among many possible forms, as

$$\varphi_2(x,y) = U_2 \int_0^\infty \cosh\left[\lambda\beta_2(y+b)\right] \cdot \left[E_2(\lambda) \sin \lambda x + F_2(\lambda) \cos \lambda x\right] d\lambda + U_2 \int_0^\infty \sinh\left[\lambda\beta_2(y+b)\right] \cdot \left[G_2(\lambda) \sin \lambda x + H_2(\lambda) \cos \lambda x\right] d\lambda \quad \text{(B13)}$$

where $E_2(\lambda)$, $F_2(\lambda)$, $G_2(\lambda)$, and $H_2(\lambda)$ are also undetermined Fourier coefficients. Then, by retracing the steps just taken for the supersonic case, there is obtained

$$u_2(x,y) = U_2 \int_0^\infty \cosh\left[\lambda\beta_2(y+b)\right] \cdot \left[E_2(\lambda) \cos \lambda x - F_2(\lambda) \sin \lambda x\right]\lambda\, d\lambda + U_2 \int_0^\infty \sinh\left[\lambda\beta_2(y+b)\right] \cdot \left[G_2(\lambda) \cos \lambda x - H_2(\lambda) \sin \lambda x\right]\lambda\, d\lambda \quad \text{(B14)}$$

and

$$v_2(x,y) = U_2\beta_2 \int_0^\infty \sinh\left[\lambda\beta_2(y+b)\right] \cdot \left[E_2(\lambda) \sin \lambda x + F_2(\lambda) \cos \lambda x\right]\lambda\, d\lambda + U_2\beta_2 \int_0^\infty \cosh\left[\lambda\beta_2(y+b)\right] \cdot \left[G_2(\lambda) \sin \lambda x + H_2(\lambda) \cos \lambda x\right]\lambda\, d\lambda \quad \text{(B15)}$$

Boundary Conditions

In these solutions for the subsonic and supersonic streams, six unknown Fourier coefficients $A_1(\lambda)$, $B_1(\lambda)$, $E_2(\lambda)$, $F_2(\lambda)$, $G_2(\lambda)$, and $H_2(\lambda)$ exist. However, these coefficients are determinable by boundary conditions at the upper and lower interfaces. The physical conditions which must be satisfied across these interfaces are: (1) equal static pressure, and (2) equal inclination of the flow. At the upper interface, condition (1) gives, in the small perturbation approximation,

$$\text{(I)} \quad -\rho_1 U_1 u_{1,y=+0} = -\rho_2 U_2 u_{2,y=-0} \text{ for all } x \tag{B16}$$

At the lower interface, the perturbation pressure is taken to be zero; condition (1) therefore reduces to

$$\text{(II)} \quad u_{2,y=-b} = 0 \text{ for all } x \tag{B17}$$

Condition (2) gives no information at the lower interface since the flow speed is zero below the interface; at the upper interface, this condition yields (small perturbation approximation)

$$\text{(III)} \quad v_{2,y=-0}\, U_1 = v_{1,y=+0}\, U_2 \text{ for all } x \tag{B18}$$

Establishment of the four equations for the four Fourier coefficients. - With use of equation (B14), boundary condition II implies

$$U_2 \int_0^\infty \left[E_2(\lambda) \cos \lambda x - F_2(\lambda) \sin \lambda x\right] \lambda \, d\lambda = 0 \tag{B19}$$

so that $E_2(\lambda)$ and $F_2(\lambda)$ vanish identically and φ_2 reduces to

$$\varphi_2 = U_2 \int_0^\infty \sinh\left[\lambda\beta_2(y+b)\right] \left[G_2(\lambda) \sin \lambda x + H_2(\lambda) \cos \lambda x\right] d\lambda \tag{B20}$$

whence

$$u_2 = U_2 \int_0^\infty \sinh\left[\lambda\beta_2(y+b)\right] \left[\lambda G_2(\lambda) \cos \lambda x - \lambda H_2(\lambda) \sin \lambda x\right] d\lambda \tag{B21}$$

and

$$v_2 = U_2\beta_2 \int_0^\infty \cosh\left[\lambda\beta_2(y+b)\right] \left[\lambda G_2(\lambda) \sin \lambda x + \lambda H_2(\lambda) \cos \lambda x\right] d\lambda \tag{B22}$$

Substituting equations (B10) and (B21), the latter evaluated at $y = -0$, into equation (B16), that is, boundary condition I, gives

$$\rho_1 U_1^2 \left\{ \frac{-\varepsilon}{\pi\beta_1} \int_0^\infty \left(\frac{\gamma}{\gamma^2 + \lambda^2} \cos \lambda x + \frac{\lambda}{\gamma^2 + \lambda^2} \sin \lambda x \right) d\lambda + \int_0^\infty \left[\lambda A_1(\lambda) \cos \lambda x - \lambda B_1(\lambda) \sin \lambda x \right] d\lambda \right\}$$

$$= \rho_2 U_2^2 \int_0^\infty \sinh (\lambda b \beta_2) \left[\lambda G_2(\lambda) \cos \lambda x - \lambda H_2(\lambda) \sin \lambda x \right] d\lambda \tag{B23}$$

whence, upon equating corresponding Fourier coefficients and making use of the fact that

$$\frac{\rho_2 U_2^2}{\rho_1 U_1^2} = \frac{M_2^2}{M_1^2} \quad \text{for} \quad p_1 = p_2 \tag{B24}$$

there is obtained

$$A_1(\lambda) - G_2(\lambda) \frac{M_2^2}{M_1^2} \sinh (\lambda b \beta_2) = \frac{\varepsilon}{\pi\beta_1} \frac{\gamma}{\gamma^2 + \lambda^2} \frac{1}{\lambda} \tag{B25}$$

and

$$B_1(\lambda) - H_2(\lambda) \frac{M_2^2}{M_1^2} \sinh (\lambda b \beta_2) = \frac{-\varepsilon}{\pi\beta_1} \frac{1}{\gamma^2 + \lambda^2} \tag{B26}$$

Similarly, boundary condition III (equation (B18)) implies

$$U_1 U_2 \beta_2 \int_0^\infty \cosh (\lambda b \beta_2) \left[\lambda G_2(\lambda) \sin \lambda x + \lambda H_2(\lambda) \cos \lambda x \right] d\lambda$$

$$= U_1 U_2 \left\{ \left(\frac{-\varepsilon}{\pi} \right) \int_0^\infty \left(\frac{\gamma}{\gamma^2 + \lambda^2} \cos \lambda x + \frac{\lambda}{\gamma^2 + \lambda^2} \sin \lambda x \right) d\lambda - \beta_1 \int_0^\infty \left[\lambda A_1(\lambda) \cos \lambda x - \lambda B_1(\lambda) \sin \lambda x \right] d\lambda \right\} \tag{B27}$$

so that

$$A_1(\lambda) + H_2(\lambda) \frac{\beta_2}{\beta_1} \cosh (\lambda b \beta_2) = \frac{-\varepsilon}{\pi\lambda\beta_1} \frac{\gamma}{\gamma^2 + \lambda^2} \tag{B28}$$

and

$$B_1(\lambda) - G_2(\lambda)\frac{\beta_2}{\beta_1}\cosh(\lambda b\beta_2) = \frac{\varepsilon}{\pi\beta_1}\frac{1}{\gamma^2+\lambda^2} \tag{B29}$$

Hence, the problem is now reduced to one of evaluating the four undetermined Fourier coefficients, $A_1(\lambda)$, $B_1(\lambda)$, $G_2(\lambda)$, and $H_2(\lambda)$ by means of the four equations (B25), (B26), (B28), and (B29).

Evaluation of Fourier Coefficients

Solving equations (B25), (B26), (B28), and (B29) simultaneously yields the following expressions for $G_2(\lambda)$ and $H_2(\lambda)$:

$$G_2(\lambda)\left[\left(\frac{M_2^2}{M_1^2}\right)^2\sinh^2(\lambda b\beta_2) + \frac{\beta_2^2}{\beta_1^2}\cosh^2(\lambda b\beta_2)\right]$$

$$= \frac{-2\varepsilon}{\pi\beta_1}\cdot\frac{1}{\gamma^2+\lambda^2}\left[\frac{\gamma}{\lambda}\left(\frac{M_2^2}{M_1^2}\right)\sinh(\lambda b\beta_2) + \frac{\beta_2}{\beta_1}\cosh(\lambda b\beta_2)\right] \tag{B30}$$

and

$$H_2(\lambda)\left[\frac{\beta_2^2}{\beta_1^2}\cosh^2(\lambda b\beta_2) + \left(\frac{M_2^2}{M_1^2}\right)^2\sinh^2(\lambda b\beta_2)\right]$$

$$= \frac{-2\varepsilon}{\pi\beta_1}\cdot\frac{1}{\gamma^2+\lambda^2}\left[\frac{\beta_2}{\beta_1}\frac{\gamma}{\lambda}\cosh(\lambda b\beta_2) - \frac{M_2^2}{M_1^2}\sinh(\lambda b\beta_2)\right] \tag{B31}$$

In addition, if the Mach number parameter θ is defined such that[a]

$$\cos\frac{\theta}{2} = \frac{\dfrac{M_2^2}{M_1^2}}{\sqrt{\left(\dfrac{M_2^2}{M_1^2}\right)^2 + \dfrac{\beta_2^2}{\beta_1^2}}} \tag{B32}$$

---

[a]Although simplicity is not necessarily thereby achieved, θ is introduced so as to maintain a parallel presentation with that of reference 2.

then

$$\left(\frac{M_2^2}{M_1^2}\right)^2 \sinh^2(\lambda b\beta_2) + \frac{\beta_2^2}{\beta_1^2}\cosh^2(\lambda b\beta_2) = \frac{1}{2}\left(\frac{M_2^2}{M_1^2}\right)^2 \frac{\cosh(2\lambda b\beta_2) - \cos\theta}{\cos^2\frac{\theta}{2}} \tag{B33}$$

so that $G_2(\lambda)$ and $H_2(\lambda)$ are also given by

$$G_2(\lambda)\left[\frac{1}{2}\left(\frac{M_2^2}{M_1^2}\right)^2 \frac{\cosh(2\lambda b\beta_2) - \cos\theta}{\cos^2\frac{\theta}{2}}\right]$$

$$= \frac{-2\varepsilon}{\pi\beta_1}\cdot\frac{1}{\gamma^2 + \lambda^2}\left[\frac{\gamma}{\lambda}\left(\frac{M_2^2}{M_1^2}\right)\sinh(\lambda b\beta_2) + \frac{\beta_2}{\beta_1}\cosh(\lambda b\beta_2)\right] \tag{B34}$$

and

$$H_2(\lambda)\left[\frac{1}{2}\left(\frac{M_2^2}{M_1^2}\right)\frac{\cosh(2\lambda b\beta_2) - \cos\theta}{\cos^2\frac{\theta}{2}}\right]$$

$$= \frac{-2\varepsilon}{\pi\beta_1}\cdot\frac{1}{\gamma^2 + \lambda^2}\left[\frac{\beta_2}{\beta_1}\frac{\gamma}{\lambda}\cosh(\lambda b\beta_2) - \frac{M_2^2}{M_1^2}\sinh(\lambda b\beta_2)\right] \tag{B35}$$

Similarly, by means of the same equations, the following expressions for $A_1(\lambda)$ and $B_1(\lambda)$ are also obtained:

$$A_1(\lambda)\left[\frac{\beta_2^2}{\beta_1^2}\cosh^2(\lambda b\beta_2) + \left(\frac{M_2^2}{M_1^2}\right)^2\sinh^2(\lambda b\beta_2)\right]$$

$$= \frac{\varepsilon}{\pi\beta_1}\frac{1}{\gamma^2 + \lambda^2}\left[\frac{\beta_2^2}{\beta_1^2}\frac{\gamma}{\lambda}\cosh^2(\lambda b\beta_2) - \left(\frac{M_2^2}{M_1^2}\right)^2\frac{\gamma}{\lambda}\sinh^2(\lambda b\beta_2) - 2\frac{M_2^2}{M_1^2}\frac{\beta_2}{\beta_1}\sinh(\lambda b\beta_2)\cosh(\lambda b\beta_2)\right] \tag{B36}$$

and

$$B_1(\lambda)\left[\left(\frac{M_2^2}{M_1^2}\right)^2 \sinh^2(\lambda b\beta_2) + \frac{\beta_2^2}{\beta_1^2}\cosh^2(\lambda b\beta_2)\right]$$

$$= \frac{-\varepsilon}{\pi\beta_1}\frac{1}{\gamma^2+\lambda^2}\left[2\frac{\gamma}{\lambda}\frac{M_2^2}{M_1^2}\frac{\beta_2}{\beta_1}\sinh(\lambda b\beta_2)\cosh(\lambda b\beta_2) - \left(\frac{M_2^2}{M_1^2}\right)^2 \sinh^2(\lambda b\beta_2) + \frac{\beta_2^2}{\beta_1^2}\cosh^2(\lambda b\beta_2)\right] \tag{B37}$$

Solution for Pressure Along Upper Interface

With the Fourier coefficients $A_1(\lambda)$, $B_1(\lambda)$, $G_2(\lambda)$, and $H_2(\lambda)$ evaluated, the solution of the originally stated problem is now complete. However, there exist other quantities of interest such as the pressure distribution along the upper interface and also the displacement of each interface from its undisturbed position. These quantities will now be considered.

If the change in pressure from the undisturbed value is denoted by Δp, then the linearized value is

$$\Delta p = -\rho U u$$

Hence, denoting quantities at the upper interface by the subscript U and those at the lower interface by the subscript L, equation (B21) and boundary condition I give

$$(\Delta p)_U = -\rho_2 U_2 u_{2,y=-0} = -\rho_2 U_2^2 \int_0^\infty \sinh(\lambda b\beta_2)\left[\lambda G_2(\lambda)\cos\lambda x - \lambda H_2(\lambda)\sin\lambda x\right] d\lambda \tag{B38}$$

where $G_2(\lambda)$ and $H_2(\lambda)$ are given by equations (B34) and (B35). Or, with use of equation (B24) and also since equation (B32) further implies

$$\cos\theta \equiv 2\cos^2\frac{\theta}{2} - 1 = \frac{\left(\frac{M_2^2}{M_1^2}\right)^2 - \frac{\beta_2^2}{\beta_1^2}}{\left(\frac{M_1^2}{M_1^2}\right)^2 + \frac{\beta_2^2}{\beta_1^2}} \tag{B39}$$

and

$$\sin\frac{\theta}{2} \equiv \sqrt{1 - \cos^2\frac{\theta}{2}} = \frac{\frac{\beta_2}{\beta_1}}{\sqrt{\left(\frac{M_2^2}{M_1^2}\right)^2 + \frac{\beta_2^2}{\beta_1^2}}} \tag{B40}$$

equation (B38) can then be written as

$$\frac{(\Delta p)_U}{\frac{1}{2}\rho_1 U_1^2} = \frac{4\varepsilon}{\pi\beta_1}\left[\cos^2\frac{\theta}{2}\int_0^\infty \left(\frac{\gamma}{\gamma^2+\lambda^2}\cos\lambda x + \frac{\lambda}{\gamma^2+\lambda^2}\sin\lambda x\right) d\lambda - \right.$$

$$\frac{1}{2}\sin^2\theta \int_0^\infty \frac{\gamma\cos\lambda x + \lambda\sin\lambda x}{(\gamma^2+\lambda^2)(\cosh 2\lambda b\beta_2 - \cos\theta)}\, d\lambda +$$

$$\left.\frac{1}{2}\sin\theta \int_0^\infty \frac{\lambda\sinh(2\lambda b\beta_2)\cos\lambda x - \gamma\sinh(2\lambda b\beta_2)\sin\lambda x}{(\gamma^2+\lambda^2)(\cosh 2\lambda b\beta_2 - \cos\theta)}\, d\lambda\right] \tag{B41}$$

Limit as $\gamma \to 0$ (incoming waves → step function). - If $\gamma \to 0$, the incoming waves will degenerate into a single compression wave with deflection angle ε. Consequently, in order to obtain the value of the pressure change at the upper interface for a single compression wave of deflection angle ε, let $\gamma \to 0$ in the expression for $\frac{(\Delta p)_U}{\frac{1}{2}\rho_1 U_1^2}$.

From equation (B8)[a]

[a]Here, the subscripts under I designate the various integrals rather than any position in a subsonic or supersonic stream.

$$I_1 \equiv \int_0^\infty \left(\frac{\gamma}{\gamma^2 + \lambda^2} \cos \lambda x + \frac{\lambda}{\gamma^2 + \lambda^2} \sin \lambda x \right) d\lambda = \begin{cases} 0 , & x < 0 \\ \frac{\pi}{2} , & x = 0 \\ \pi e^{-\gamma x} , & x > 0 \end{cases} \tag{B42}$$

whence

$$\lim_{\gamma \to 0} \int_0^\infty \left(\frac{\gamma}{\gamma^2 + \lambda^2} \cos \lambda x + \frac{\lambda}{\gamma^2 + \lambda^2} \sin \lambda x \right) d\lambda = \begin{cases} 0 , & x < 0 \\ \frac{\pi}{2} , & x = 0 \\ \pi , & x > 0 \end{cases} \tag{B43}$$

For the other integrals of equation (B41), a theorem justifying the interchange of the processes of integration and of passing to a limit is necessary. One such appropriate theorem which will suffice for the analysis in this report will now be stated (reference 10, p. 474).

DEFINITION. - Let $R = (a \infty \alpha\beta)$ denote the rectangle determined by $a \leq x \leq \infty$, $\alpha \leq t \leq \beta$, β finite or infinite. The function $f(x,t)$ is said to be REGULAR IN R when: (1) $f(x,t)$ has no point of infinite discontinuity in R; (2) $f(x,t)$ is integrable in $a \leq x \leq \infty$ for each t in $\alpha \leq t \leq \beta$.

THEOREM I. - (1) Let $f(x,t)$ be regular in $R = (a \infty \alpha\beta)$, β finite or infinite, except possibly on the lines $x = a_1, \ldots, x = a_r$. (2) Let

$$\int_a^\infty f(x,t)dx$$

be uniformly convergent in $\alpha \leq t \leq \beta$. (3) As $t \to t_0$, t_0 finite or infinite, let $f(x,t)$ approach a limiting function $F(x)$ uniformly in any region $a \leq x \leq b$, except possibly on the lines $x = a_1, \ldots, x = a_r$.

Then,

$$\lim_{t \to t_0} \int_a^\infty f(x,t)\, dx \quad \text{exists.}$$

(4) Let $F(x)$ be integrable in any region $a \leq x \leq b$.

Then,

$$\lim_{t \to t_0} \int_a^{\infty} f(x,t)dx = \int_a^{\infty} F(x)dx$$

Thus, for

$$I_2 \equiv \int_0^{\infty} \frac{\gamma \cos \lambda x}{(\gamma^2 + \lambda^2)(\cosh 2b\lambda\beta_2 - \cos \theta)} d\lambda \qquad \text{(B44)}$$

first letting $z = \lambda/\gamma$ so that

$$I_2 = \int_0^{\infty} \frac{\cos (\gamma x z)}{(z^2 + 1)(\cosh 2b\gamma z\beta_2 - \cos \theta)} dz \qquad \text{(B45)}$$

and then applying theorem I, there is obtained

$$\lim_{\gamma \to 0} I_2 = \frac{1}{1 - \cos \theta} \int_0^{\infty} \frac{dz}{z^2 + 1} = \frac{\pi}{2(1 - \cos \theta)} \equiv \frac{\pi}{4 \sin^2 \frac{\theta}{2}} \qquad \text{(B46)}$$

For

$$I_3 \equiv \int_0^{\infty} \frac{\lambda \sin \lambda x}{(\gamma^2 + \lambda^2)(\cosh 2b\beta_2\lambda - \cos \theta)} d\lambda \qquad \text{(B47)}$$

and

$$I_4 \equiv \int_0^{\infty} \frac{\lambda \sinh(2b\beta_2\lambda) \cos \lambda x}{(\gamma^2 + \lambda^2)(\cosh 2b\beta_2\lambda - \cos \theta)} d\lambda \qquad \text{(B48)}$$

let

$$S = 2b\lambda\beta_2 \tag{B49}$$

$$\xi = \frac{\pi x}{2b\beta_2} \tag{B50}$$

so that

$$I_3 = \int_0^\infty \frac{S \sin \frac{S\xi}{\pi}}{\left(\gamma^2 + \frac{S^2}{4b^2\beta_2{}^2}\right)(\cosh S - \cos\theta)}\, dS \tag{B51}$$

and

$$I_4 = \int_0^\infty \frac{S \sinh S \cos \frac{S\xi}{\pi}}{\left(\gamma^2 + \frac{S^2}{4b^2\beta_2{}^2}\right)(\cosh S - \cos\theta)}\, dS \tag{B52}$$

Then,

$$\lim_{\gamma \to 0} I_3 = \int_0^\infty \frac{\sin \frac{S\xi}{\pi}}{S(\cosh S - \cos\theta)}\, dS \tag{B53}$$

and

$$\lim_{\gamma \to 0} I_4 = \int_0^\infty \frac{\sinh S \cos \frac{S\xi}{\pi}}{S(\cosh S - \cos\theta)}\, dS \tag{B54}$$

Lastly,

$$\lim_{\gamma \to 0} I_5 \equiv \lim_{\gamma \to 0} \int_0^\infty \frac{\gamma \sinh(2\lambda b\beta_2)\sin \lambda x}{(\gamma^2 + \lambda^2)(\cosh 2\lambda b\beta_2 - \cos\theta)}\, d\lambda \equiv 0 \tag{B55}$$

Solution for single incoming compressive wave. - Combining these five limits yields

$$\lim_{\gamma \to 0} \frac{(\Delta p)_U}{\frac{1}{2}\rho_1 U_1^2} = \frac{-4\varepsilon}{\beta_1}\left[\cos^2\frac{\theta}{2}\cdot 1(\xi) - \frac{1}{2}\sin^2\theta\left(\frac{1}{4\sin^2\frac{\theta}{2}}\right) - \right.$$

$$\left. \frac{1}{2\pi}\sin^2\theta\int_0^\infty \frac{\sin\frac{S\xi}{\pi}}{S(\cosh S - \cos\theta)}\,dS + \frac{1}{2\pi}\sin\theta\int_0^\infty \frac{\sinh S\cos\frac{S\xi}{\pi}}{S(\cosh S - \cos\theta)}\,dS\right] \tag{B56}$$

where $1(\xi)$ is defined by

$$1(\xi) \equiv \begin{cases} 0, & \xi < 0 \\ \frac{1}{2}, & \xi = 0 \\ 1, & \xi > 0 \end{cases} \tag{B57}$$

Now, it can be shown by contour integration that, for $\xi > 0$,

$$\frac{1}{2\pi}\int_0^\infty \frac{\sin\frac{S\xi}{\pi}}{S(\cosh S - \cos\theta)}\,dS = \frac{1}{8\sin^2\frac{\theta}{2}} + \frac{1}{2\pi\sin\theta}\sum_{n=0}^{\infty} e^{-(2n+1)\xi}\left[\frac{e^{-\left(\frac{\pi-\theta}{\pi}\right)\xi}}{2n+2-\frac{\theta}{\pi}} - \frac{e^{\left(\frac{\pi-\theta}{\pi}\right)\xi}}{2n+\frac{\theta}{\pi}}\right], \quad \xi > 0 \tag{B58}$$

and

$$\frac{1}{2\pi}\int_0^\infty \frac{\sinh S\cos\frac{S\xi}{\pi}}{S(\cosh S - \cos\theta)}\,dS = \frac{1}{2\pi}\sum_{n=0}^{\infty} e^{-(2n+1)\xi}\left[\frac{e^{-\left(\frac{\pi-\theta}{\pi}\right)\xi}}{2n+2-\frac{\theta}{\pi}} + \frac{e^{\left(\frac{\pi-\theta}{\pi}\right)\xi}}{2n+\frac{\theta}{\pi}}\right], \quad \xi > 0 \tag{B59}$$

Furthermore, since the integrands are odd and even functions of ξ, respectively, it can immediately be deduced that, for $\xi < 0$,

$$\frac{1}{2\pi}\int_0^\infty \frac{\sin\frac{S\xi}{\pi}}{S(\cosh S - \cos\theta)}\,dS = \frac{-1}{8\sin^2\frac{\theta}{2}} - \frac{1}{2\pi\sin\theta}\sum_{n=0}^{\infty} e^{(2n+1)\xi}\left[\frac{e^{\left(\frac{\pi-\theta}{\pi}\right)\xi}}{2n+2-\frac{\theta}{\pi}} - \frac{e^{-\left(\frac{\pi-\theta}{\pi}\right)\xi}}{2n+\frac{\theta}{\pi}}\right], \quad \xi < 0 \tag{B60}$$

and

$$\frac{1}{2\pi}\int_0^\infty \frac{\sinh S \cos\frac{S\xi}{\pi}}{S(\cosh S - \cos\theta)}\,dS = \frac{1}{2\pi}\sum_{n=0}^{\infty} e^{(2n+1)\xi}\left[\frac{e^{\left(\frac{\pi-\theta}{\pi}\right)\xi}}{2n+2-\frac{\theta}{\pi}} + \frac{e^{-\left(\frac{\pi-\theta}{\pi}\right)\xi}}{2n+\frac{\theta}{\pi}}\right], \quad \xi<0 \tag{B61}$$

Therefore, with the substitution of these results into equation (B56), it follows that:

$$\lim_{\gamma\to 0}\frac{(\Delta p)_U}{\frac{1}{2}\rho_1 U_1^2} = \begin{cases} \dfrac{4\varepsilon}{\pi\beta_1}\sin\theta\displaystyle\sum_{n=0}^{\infty}\frac{e^{\left(2n+2-\frac{\theta}{\pi}\right)\xi}}{2n+2-\frac{\theta}{\pi}}, & \xi<0 \qquad \text{(B62)} \\ \dfrac{4\varepsilon}{\pi\beta_1}\sin\theta\displaystyle\sum_{n=0}^{\infty}\frac{e^{-\left(2n+2-\frac{\theta}{\pi}\right)\xi}}{2n+\frac{\theta}{\pi}}, & \xi>0 \qquad \text{(B63)} \end{cases}$$

Displacement of Upper Interface

A quantity of primary interest is the shape of the distorted interface between the supersonic and the subsonic flows. The slope of this interface is related very simply to the already determined pressure at the interface, according to the following considerations. If the displacement from the undisturbed position is denoted by η_U, this slope is given by

$$\frac{d\eta_U}{dx} \cong \frac{v_2}{U_2} \qquad \text{all } \xi,\ y = 0 \tag{B73}$$

approximately. Now, applying the boundary condition of equal slopes on both sides of the interface, equation (B18) gives

$$\frac{v_2}{U_2} = \frac{v_1}{U_1} \qquad \text{all } \xi,\ y = 0 \tag{B74}$$

Furthermore, v_1 can be related to u_1. In the region $\xi < 0$, only outgoing waves exist, corresponding to the g-function in equation (B2); thus by differentiation of g,

$$v_1 = - \beta_1 u_1 \qquad \xi < 0,\ y = 0 \tag{B75a}$$

In the region $\xi > 0$, there exists, in addition, the incoming weak shock providing a flow deflection ε for $\gamma \to 0$, corresponding to the f-function in equation (B2); this provides an additional term such that

$$\lim_{\gamma \to 0} v_1 = - \beta_1 u_1 - 2\varepsilon U_1 \qquad \xi > 0,\ y = 0 \tag{B75b}$$

When these equations are combined, there results

$$\lim_{\gamma \to 0} \frac{d\eta_U}{dx} = \begin{cases} - \beta_1 \dfrac{u_1}{U_1}, & \xi < 0,\ y = 0 \\ - \beta_1 \dfrac{u_1}{U_1} - 2\varepsilon, & \xi > 0,\ y = 0 \end{cases} \tag{B76}$$

Then, by virtue of the relation $\Delta p_U = - \rho_1 U_1 u_1$, this may be written

$$\lim_{\gamma \to 0} \frac{d\eta_U}{dx} = \begin{cases} \dfrac{1}{2} \beta_1 \left(\dfrac{\Delta p_U}{\frac{1}{2} \rho_1 U_1^2} \right), & \xi < 0,\ y = 0 \\ \dfrac{1}{2} \beta_1 \left(\dfrac{\Delta p_U}{\frac{1}{2} \rho_1 U_1^2} \right) - 2\varepsilon, & \xi > 0,\ y = 0 \end{cases} \tag{B77}$$

This is the desired relation between the local slope and the pressure of the interface.

Upon substitution of the calculated pressure, equations (B62) and (B63), there results

$$\lim_{\gamma \to 0} \frac{d\eta_U}{dx} = \begin{cases} \dfrac{2\varepsilon}{\pi} \sin\theta \displaystyle\sum_{n=0}^{\infty} \frac{e^{\left(2n+2 - \frac{\theta}{\pi}\right)\xi}}{2n + \frac{\theta}{\pi}}, & \xi < 0 \qquad \text{(B78)} \\ 2\varepsilon \left(\dfrac{\sin\theta}{\pi} \displaystyle\sum_{n=0}^{\infty} \frac{e^{-\left(2n + \frac{\theta}{\pi}\right)\xi}}{2n + \frac{\theta}{\pi}} - 1 \right), & \xi > 0 \qquad \text{(B79)} \end{cases}$$

Expressions for displacement of upper interface. - Denoting $\lim_{\gamma \to 0} \frac{d\eta_U}{dx}$ by $\frac{d\eta_U^*}{dx}$, equation (B50) gives

$$\frac{d\eta_U^*}{dx} = \frac{d\eta_U^*}{d\xi} \frac{d\xi}{dx} = \frac{d\eta_U^*}{d\xi} \cdot \frac{\pi}{2b\beta_2} \tag{B80}$$

Thus, with the assumption that

$$\eta_U^*(-\infty;\ \theta) = 0 \tag{B81}$$

the expressions for $\frac{d\eta_U^*}{dx}$ can be integrated and will yield

$$\frac{\pi}{2b\beta_2} \eta_U^*(\xi;\ \theta) = \frac{2\varepsilon}{\pi} \sin\theta \sum_{n=0}^{\infty} \frac{e^{\left(2n+2 - \frac{\theta}{\pi}\right)\xi}}{\left(2n+2 - \frac{\theta}{\pi}\right)^2}, \qquad \xi < 0 \tag{B82}$$

while for $\xi > 0$, since

$$\eta_U^*(\xi;\ \theta) = \int_{-\infty}^{-0} \frac{d\eta_U^*(\xi<0;\ \theta)}{d\xi} d\xi + \int_{+0}^{\xi} \frac{d\eta_U^*(\xi>0;\ \theta)}{d\xi} d\xi \tag{B83}$$

there is obtained

$$\eta_U^*(\xi;\ \theta) = \frac{2\varepsilon}{\pi} \sin\theta \sum_{n=0}^{\infty} \frac{1}{\left(2n+2 - \frac{\theta}{\pi}\right)^2} - 2\varepsilon \left[\frac{\sin\theta}{\pi} \sum_{n=0}^{\infty} \frac{e^{-\left(2n + \frac{\theta}{\pi}\right)\xi}}{\left(2n + \frac{\theta}{\pi}\right)^2} + \xi \right]_{+0}^{\xi} \tag{B84}$$

Hence

$$\eta_U^*(\xi;\ \theta) = \frac{2\varepsilon}{\pi} \sin\theta \sum_{n=0}^{\infty} \left[\frac{1}{\left(2n+2 - \frac{\theta}{\pi}\right)^2} + \frac{1}{\left(2n + \frac{\theta}{\pi}\right)^2} - \frac{e^{-\left(2n + \frac{\theta}{\pi}\right)\xi}}{\left(2n + \frac{\theta}{\pi}\right)^2} \right] - 2\varepsilon\xi, \qquad \xi > 0 \tag{B85}$$

Therefore, in summary,

$$\frac{\pi}{2b\beta_2}\eta_U^*(\xi;\theta) = \begin{cases} \dfrac{2\varepsilon}{\pi}\sin\theta\displaystyle\sum_{n=0}^{\infty}\dfrac{e^{\left(2n+2-\frac{\theta}{\pi}\right)\xi}}{\left(2n+2-\frac{\theta}{\pi}\right)^2}, & \xi<0 \qquad \text{(B82)} \\ \dfrac{2\varepsilon}{\pi}\sin\theta\displaystyle\sum_{n=0}^{\infty}\left[\dfrac{1}{\left(2n+2-\frac{\theta}{\pi}\right)^2}+\dfrac{1}{\left(2n+\frac{\theta}{\pi}\right)^2}-\dfrac{e^{-\left(2n+\frac{\theta}{\pi}\right)\xi}}{\left(2n+\frac{\theta}{\pi}\right)^2}\right]-2\varepsilon\xi, & \xi>0 \qquad \text{(B85)} \end{cases}$$

By inspection of equations (B82) and (B85), it is noted that $\eta_U^*(\xi;\theta)$ is finite and continuous at $\xi = 0$, while, on the other hand, equations (B78) and (B79) show that $d\eta_U^*/dx$ is infinite at $\xi = 0$.

Displacement of Lower Interface

Finally, the expression for the displacement of the lower interface will be derived. If the displacement from the undisturbed position is denoted by η_L, this displacement will have a slope given in linearized approximation by

$$\frac{d\eta_L}{dx} = \frac{v_{2,y=-b}}{U_2} \qquad \text{(B86)}$$

or, with use of equation (B22),

$$\frac{d\eta_L}{dx} = \int_0^{\infty}\lambda\beta_2\left[G_2(\lambda)\sin\lambda x + H_2(\lambda)\cos\lambda x\right]d\lambda \qquad \text{(B87)}$$

where $G_2(\lambda)$ and $H_2(\lambda)$ are given by equations (B34) and (B35). That is,

$$\frac{d\eta_L}{dx} = \frac{-\frac{2\epsilon}{\pi}\frac{\beta_2}{\beta_1}\cos^2\frac{\theta}{2}}{\left(\frac{M_2^2}{M_1^2}\right)^2}\int_0^\infty \frac{\left(\gamma\frac{M_2^2}{M_1^2}\sinh\lambda b\beta_2 + \lambda\frac{\beta_2}{\beta_1}\cosh\lambda b\beta_2\right)\sin\lambda x}{(\gamma^2+\lambda^2)\frac{1}{2}(\cosh 2\lambda b\beta_2 - \cos\theta)}\,d\lambda +$$

$$\frac{\frac{2\epsilon}{\pi}\frac{\beta_2}{\beta_1}\cos^2\frac{\theta}{2}}{\left(\frac{M_2^2}{M_1^2}\right)^2}\int_0^\infty \frac{\left(-\gamma\frac{\beta_2}{\beta_1}\cosh\lambda b\beta_2 + \lambda\frac{M_2^2}{M_1^2}\sinh\lambda b\beta_2\right)\cos\lambda x}{(\gamma^2+\lambda^2)\frac{1}{2}(\cosh 2\lambda b\beta_2 - \cos\theta)}\,d\lambda \qquad \text{(B88)}$$

Limit as $\gamma \to 0$ (incoming wave → step function). - Consideration will now be given the various parts of the expression for $d\eta_U/dx$ as one again passes to the limit $\gamma = 0$. For

$$I_6 \equiv \int_0^\infty \frac{\gamma \sinh(\lambda b\beta_2)\sin\lambda x}{(\gamma^2+\lambda^2)(\cosh 2b\lambda\beta_2 - \cos\theta)}\,d\lambda \qquad \text{(B89)}$$

first letting $\lambda = \gamma z$, there is obtained

$$\lim_{\gamma\to 0} I_6 = \lim_{\gamma\to 0}\int_0^\infty \frac{\sinh(\gamma bz\beta_2)\cdot\sin(\gamma xz)}{(1+z^2)(\cosh 2\gamma zb\beta_2 - \cos\theta)}\,dz \equiv 0 \qquad \text{(B90)}$$

Similarly, for

$$I_7 \equiv \int_0^\infty \frac{\gamma\cosh(\lambda b\beta_2)\cos\lambda x}{(\gamma^2+\lambda^2)(\cosh 2\lambda b\beta_2 - \cos\theta)}\,d\lambda \qquad \text{(B91)}$$

$$\lim_{\gamma\to 0} I_7 = \lim_{\gamma\to 0}\int_0^\infty \frac{\cosh(\gamma zb\beta_2)\cos(\gamma zx)}{(1+z^2)(\cosh 2\gamma zb\beta_2 - \cos\theta)}\,dz \qquad \text{(B92)}$$

$$= \frac{1}{1-\cos\theta}\int_0^\infty \frac{dz}{1+z^2} = \frac{1}{1-\cos\theta}\cdot\frac{\pi}{2}$$

so that

$$\lim_{\gamma \to 0} I_7 = \frac{\pi}{4 \sin^2 \frac{\theta}{2}} \tag{B93}$$

For

$$I_8 \equiv \int_0^\infty \frac{\lambda \cosh (\lambda b \beta_2) \cdot \sin \lambda x}{(\gamma^2 + \lambda^2)(\cosh 2\lambda b \beta_2 - \cos \theta)} d\lambda \tag{B94}$$

and

$$I_9 \equiv \int_0^\infty \frac{\lambda \sinh (\lambda b \beta_2) \cdot \cos \lambda x}{(\gamma^2 + \lambda^2)(\cosh 2\lambda b \beta_2 - \cos \theta)} d\lambda \tag{B95}$$

introducing S and ξ as before yields

$$I_8 = \int_0^\infty \frac{S \cosh \frac{S}{2} \sin \frac{S\xi}{\pi}}{\left(\gamma^2 + \frac{S^2}{4b^2\beta_2^2}\right)(\cosh S - \cos \theta)} dS \tag{B96}$$

and

$$I_9 = \int_0^\infty \frac{S \sinh \frac{S}{2} \cos \frac{S\xi}{\pi}}{\left(\gamma^2 + \frac{S^2}{4b^2\beta_2^2}\right)(\cosh S - \cos \theta)} dS \tag{B97}$$

whence

$$\lim_{\gamma \to 0} I_8 = \int_0^\infty \frac{\cosh \frac{S}{2} \sin \frac{S\xi}{\pi}}{S(\cosh S - \cos \theta)} dS \tag{B98}$$

and

$$\lim_{\gamma \to 0} I_9 = \int_0^\infty \frac{\sinh \frac{S}{2} \cos \frac{S\xi}{\pi}}{S(\cosh S - \cos \theta)} dS \tag{B99}$$

Furthermore, following reference 2, it can be shown that, for $\xi > 0$,

$$\lim_{\gamma \to 0} I_8 = \begin{cases} -\dfrac{\pi}{4 \sin^2 \frac{\theta}{2}} + \dfrac{1}{2 \sin \frac{\theta}{2}} \displaystyle\sum_{n=0}^{\infty} (-1)^n e^{(2n+1)\xi} \left[\dfrac{e^{\left(\frac{\pi-\theta}{\pi}\right)\xi}}{2n + 2 - \frac{\theta}{\pi}} + \dfrac{e^{-\left(\frac{\pi-\theta}{\pi}\right)\xi}}{2n + \frac{\theta}{\pi}} \right], & \xi < 0 \quad \text{(B100)} \\ \dfrac{\pi}{4 \sin^2 \frac{\theta}{2}} - \dfrac{1}{2 \sin \frac{\theta}{2}} \displaystyle\sum_{n=0}^{\infty} (-1)^n e^{-(2n+1)\xi} \left[\dfrac{e^{-\left(\frac{\pi-\theta}{\pi}\right)\xi}}{2n + 2 - \frac{\theta}{\pi}} + \dfrac{e^{\left(\frac{\pi-\theta}{\pi}\right)\xi}}{2n + \frac{\theta}{\pi}} \right], & \xi > 0 \quad \text{(B101)} \end{cases}$$

and

$$\lim_{\gamma \to 0} I_9 = \begin{cases} -\dfrac{1}{2 \cos \frac{\theta}{2}} \displaystyle\sum_{n=0}^{\infty} (-1)^n e^{(2n+1)\xi} \left[\dfrac{e^{\left(\frac{\pi-\theta}{\pi}\right)\xi}}{2n + 2 - \frac{\theta}{\pi}} - \dfrac{e^{-\left(\frac{\pi-\theta}{\pi}\right)\xi}}{2n + \frac{\theta}{\pi}} \right], & \xi < 0 \quad \text{(B102)} \\ -\dfrac{1}{2 \cos \frac{\theta}{2}} \displaystyle\sum_{n=0}^{\infty} (-1)^n e^{-(2n+1)\xi} \left[\dfrac{e^{-\left(\frac{\pi-\theta}{\pi}\right)\xi}}{2n + 2 - \frac{\theta}{\pi}} - \dfrac{e^{\left(\frac{\pi-\theta}{\pi}\right)\xi}}{2n + \frac{\theta}{\pi}} \right], & \xi > 0 \quad \text{(B103)} \end{cases}$$

Simplification of expressions for slope. - Combining these limits and using equations (B32) and (B40) yield

$$\lim_{\gamma \to 0} \frac{d\eta_L}{dx} = -2\varepsilon \sin^2 \frac{\theta}{2} \left(\frac{1}{\sin^2 \frac{\theta}{2}} - \frac{2}{\pi \sin \frac{\theta}{2}} \sum_{n=0}^{\infty} (-1)^n \frac{e^{-\left(2n + \frac{\theta}{\pi}\right)\xi}}{2n + \frac{\theta}{\pi}} \right), \quad \xi > 0 \qquad \text{(B104)}$$

That is,

$$\lim_{\gamma \to 0} \frac{d\eta_L}{dx} = -2\varepsilon \left(1 - \frac{2}{\pi} \sin \frac{\theta}{2} \sum_{n=0}^{\infty} (-1)^n \frac{e^{-\left(2n + \frac{\theta}{\pi}\right)\xi}}{2n + \frac{\theta}{\pi}} \right), \quad \xi > 0 \qquad \text{(B105)}$$

Furthermore, by symmetry considerations of the various integrands, it follows that, for $\xi < 0$,

$$\lim_{\gamma \to 0} \frac{d\eta_L}{dx} = -2\varepsilon \sin^2 \frac{\theta}{2} \left\{ \frac{1}{\pi \sin \frac{\theta}{2}} \sum_{n=0}^{\infty} (-1)^n e^{(2n+1)\xi} \left[\frac{e^{\left(\frac{\pi-\theta}{\pi}\right)\xi}}{2n+2-\frac{\theta}{\pi}} + \frac{e^{-\left(\frac{\pi-\theta}{\pi}\right)\xi}}{2n+\frac{\theta}{\pi}} \right] + \right.$$

$$\left. \frac{1}{\pi \sin \frac{\theta}{2}} \sum_{n=0}^{\infty} (-1)^n e^{(2n+1)\xi} \left[\frac{e^{\left(\frac{\pi-\theta}{\pi}\right)\xi}}{2n+2-\frac{\theta}{\pi}} - \frac{e^{-\left(\frac{\pi-\theta}{\pi}\right)\xi}}{2n+\frac{\theta}{\pi}} \right] \right\}, \quad \xi < 0 \tag{B106}$$

That is,

$$\lim_{\gamma \to 0} \frac{d\eta_L}{dx} = -2\varepsilon \left[\frac{2}{\pi} \sin \frac{\theta}{2} \sum_{n=0}^{\infty} (-1)^n \frac{e^{\left(2n+2-\frac{\theta}{\pi}\right)\xi}}{2n+2-\frac{\theta}{\pi}} \right], \quad \xi < 0 \tag{B107}$$

Therefore, in summary,

$$\lim_{\gamma \to 0} \frac{d\eta_L}{dx} = \begin{cases} -2\varepsilon \left(\frac{2}{\pi} \sin \frac{\theta}{2} \sum_{n=0}^{\infty} (-1)^n \frac{e^{\left(2n+2-\frac{\theta}{\pi}\right)\xi}}{2n+2-\frac{\theta}{\pi}} \right), & \xi < 0 \quad \text{(B107)} \\ -2\varepsilon \left(1 - \frac{2}{\pi} \sin \frac{\theta}{2} \sum_{n=0}^{\infty} (-1)^n \frac{e^{-\left(2n+\frac{\theta}{\pi}\right)\xi}}{2n+\frac{\theta}{\pi}} \right), & \xi > 0 \quad \text{(B105)} \end{cases}$$

Final expressions for displacement of lower interface. - If $\lim_{\gamma \to 0} \frac{d\eta_L}{dx}$ is denoted by $\frac{d\eta_L^*}{dx}$, it is noted that

$$\frac{d\eta_L^*}{dx} = \frac{d\eta_L}{d\xi} \frac{d\xi}{dx} = \frac{d\eta_L^*}{d\xi} \cdot \frac{\pi}{2b\beta_2} \tag{B108}$$

so that integration of equations (B105) and (B107), along with the boundary condition

$$\eta_L^*(-\infty; \theta) = 0 \tag{B109}$$

yields, for $\xi < 0$,

$$\frac{\pi}{2b\beta_2}\eta_L^*(\xi;\theta) = -\frac{4\varepsilon}{\pi}\sin\frac{\theta}{2}\sum_{n=0}^{\infty}(-1)^n\frac{e^{\left(2n+2-\frac{\theta}{\pi}\right)\xi}}{\left(2n+2-\frac{\theta}{\pi}\right)^2}, \quad \xi < 0 \tag{B110}$$

For $\xi > 0$,

$$\eta_L^*(\xi;\theta) = \int_{-\infty}^{-0}\frac{d\eta_L^*(\xi<0;\theta)}{d\xi}d\xi + \int_{+0}^{\xi}\frac{d\eta_L^*(\xi>0;\theta)}{d\xi}d\xi$$

so that

$$\frac{\pi}{2b\beta_2}\eta_L^*(\xi;\theta) = -2\varepsilon\xi + \frac{4\varepsilon}{\pi}\sin\frac{\theta}{2}\sum_{n=0}^{\infty}(-1)^n\left[\frac{-1}{\left(2n+2-\frac{\theta}{\pi}\right)^2} + \frac{1}{\left(2n+\frac{\theta}{\pi}\right)^2} - \frac{e^{-\left(2n+\frac{\theta}{\pi}\right)\xi}}{\left(2n+\frac{\theta}{\pi}\right)^2}\right], \quad \xi > 0 \tag{B111}$$

Therefore, in summary

$$\frac{\pi}{2b\beta_2}\eta_L^*(\xi;\theta) = \begin{cases} -\frac{4\varepsilon}{\pi}\sin\frac{\theta}{2}\sum_{n=0}^{\infty}(-1)^n\frac{e^{\left(2n+2-\frac{\theta}{\pi}\right)\xi}}{\left(2n+2-\frac{\theta}{\pi}\right)^2}, & \xi < 0 \quad \text{(B110)} \\ -2\varepsilon\xi + \frac{4\varepsilon}{\pi}\sin\frac{\theta}{2}\sum_{n=0}^{\infty}(-1)^n\left[\frac{-1}{\left(2n+2-\frac{\theta}{\pi}\right)^2} + \frac{1}{\left(2n+\frac{\theta}{\pi}\right)^2} - \frac{e^{-\left(2n+\frac{\theta}{\pi}\right)\xi}}{\left(2n+\frac{\theta}{\pi}\right)^2}\right], & \xi > 0 \quad \text{(B111)} \end{cases}$$

Both $\eta_L^*(\xi;\theta)$ and $d\eta_L^*/dx$ are continuous at $\xi = 0$. The continuity of $\eta_L^*(\xi;\theta)$ is readily seen while the continuity of $d\eta_L^*/dx$ may be shown by letting $x = \theta/2\pi$ in the formula for $\pi/\sin\pi x$ given on page 208 of reference 10.

REFERENCES

1. Howarth, L.: The Propagation of Steady Disturbances in a Supersonic Stream Bounded on One Side by a Parallel Subsonic Stream. Proc. Camb. Phil. Soc., vol. 44, pt. 3, July 1948, pp. 380-390.

2. Tsien, H. S., and Finston, M.: Interaction Between Parallel Streams of Subsonic and Supersonic Velocities. Jour. Aero. Sci., vol. 16, no. 9, Sept. 1949, pp. 515-528.

3. Stewartson, K.: On the Interaction Between Shock Waves and Boundary Layers. Proc. Camb. Phil. Soc., vol. 47, pt. 3, July 1951, pp. 545-553.

4. Robinson, A.: Wave Reflection Near a Wall. Proc. Camb. Phil. Soc., vol. 47, pt. 3, July 1951, pp. 528-544.

5. Lighthill, M. J.: Reflection at a Laminar Boundary Layer of a Weak Steady Disturbance to a Supersonic Stream, Neglecting Viscosity and Heat Conduction. Quart. Jour. Mech. Appl. Math., vol. III, pt. 3, Sept. 1950, pp. 303-325.

6. Lees, Lester: Interaction Between the Laminar Boundary Layer over a Plane Surface and an Incident Oblique Shock Wave. Rep. No. 143, Aero. Eng. Lab., Princeton Univ., Jan. 24, 1949. (Office Naval Res. Contract N6ori-270, Task Order 6, Proj. NR 061-049, and Bur. Ordnance Contract Nord-7920, Task PRN-2-E.)

7. Ritter, Alfred: On the Reflection of a Weak Shock Wave from a Boundary Layer Along a Flat Plate. Ph. D. Thesis, Cornell Univ., 1951.

8. Liepmann, H. W., Roshko, A., and Dhawan, S.: On Reflection of Shock Waves from Boundary Layers. NACA TN 2334, 1951.

9. Barry, F. W., Shapiro, A. H., and Neumann, E. P.: The Interaction of Shock Waves with Boundary Layers on a Flat Surface. Jour. Aero. Sci., vol. 18, no. 4, April 1951, pp. 229-238.

10. Pierpont, James: Lectures on the Theory of Functions of Real Variables. Vol. I. Ginn & Co., 1905.

TABLE I - PERTURBATION OF UPPER INTERFACE

$\frac{\pi}{2b\beta_2}\frac{\eta_U^*}{2\epsilon}$ against $\xi = \frac{\pi x}{2b\beta_2}$ for $\theta = \pi/4$, $\pi/2$, and $3\pi/4$

ξ	$\theta=\pi/4$	$\theta=\pi/2$	$\theta=3\pi/4$
-5.0	0.00001	0.00008	0.00028
-4.0	.00007	.00035	.00097
-2.5	.00093	.00335	.00632
-1.75	.00345	.0103	.01620
-1.00	.0132	.0324	.0416
- .75	.0208	.0480	.0584
- .50	.0335	.0722	.0820
- .40	.0410	.0856	.0944
- .25	.0562	.1120	.1180
- .10	.0804	.1520	.1517
- .05	.0925	.1715	.1675
0	.1108	.1993	.1891
.01	.1138	.2009	.1856
.05	.1215	.2018	.1679
.10	.1253	.1958	.1408
.25	.1240	.1564	.0450
.40	.1169	.1003	-0.0620
.50	.1017	.0566	- .1377
.75	.0516	-0.0686	- .3363
1.00	-0.0137	- .2117	- .5450
1.75	- .2803	- .7168	-1.2120
2.50	- .6323	-1.3002	-1.9155
4.0	-1.5293	-2.6075	-3.3750
5.0	-2.2368	-3.540	-4.3650

TABLE II - PERTURBATION OF LOWER INTERFACE

$\frac{\pi}{2b\beta_2}\frac{\eta_L^*}{2\varepsilon}$ against $\xi = \frac{\pi x}{2b\beta_2}$ for $\theta = \pi/4$, $\pi/2$, and $3\pi/4$

ξ	$\theta=\pi/4$	$\theta=\pi/2$	$\theta=3\pi/4$
-5.0	-0.000013	-0.00011	-0.00073
-4.0	- .00007	- .00050	- .00254
-2.5	- .00100	- .00472	- .01653
-1.75	- .00368	- .0144	- .0420
-1.00	- .0134	- .0436	- .1057
- .75	- .0205	- .0625	- .1428
- .50	- .0309	- .0890	- .1918
- .40	- .0362	- .1021	- .2150
- .25	- .0459	- .1250	- .2550
- .10	- .0577	- .1522	- .3005
- .05	- .0622	- .1623	- .3173
0	- .0670	- .1728	- .3345
.05	- .0721	- .1841	- .3528
.10	- .0775	- .1962	- .2718
.25	- .0959	- .2358	- .4330
.40	- .1173	- .2803	- .5013
.50	- .1338	- .3130	- .5503
.75	- .1811	- .4065	- .6860
1.00	- .2389	- .5168	- .8385
1.75	- .4735	- .9293	-1.3803
2.5	- .7942	-1.4453	-2.0100
4.0	-1.6420	-2.6725	-3.4025
5.0	-2.3253	-3.5775	-4.4675

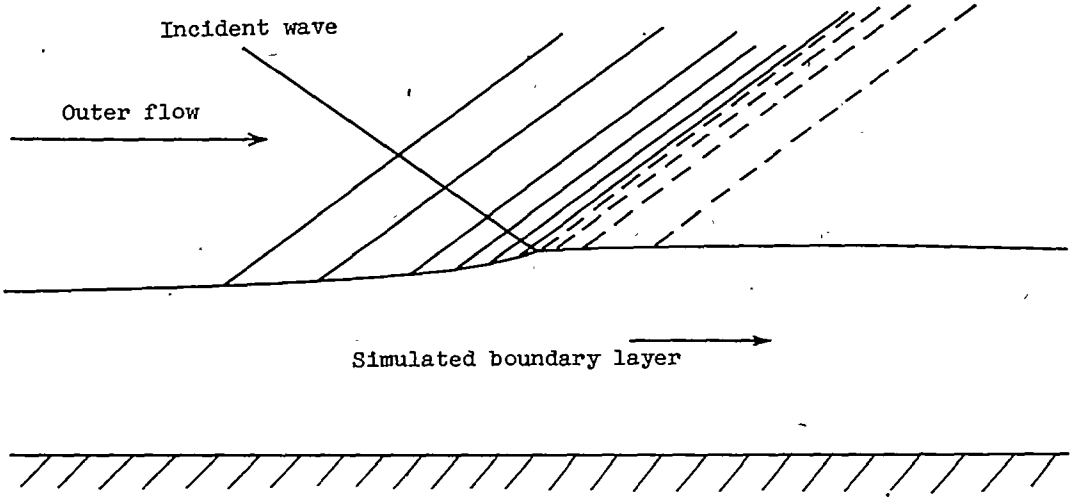

Sketch 1.

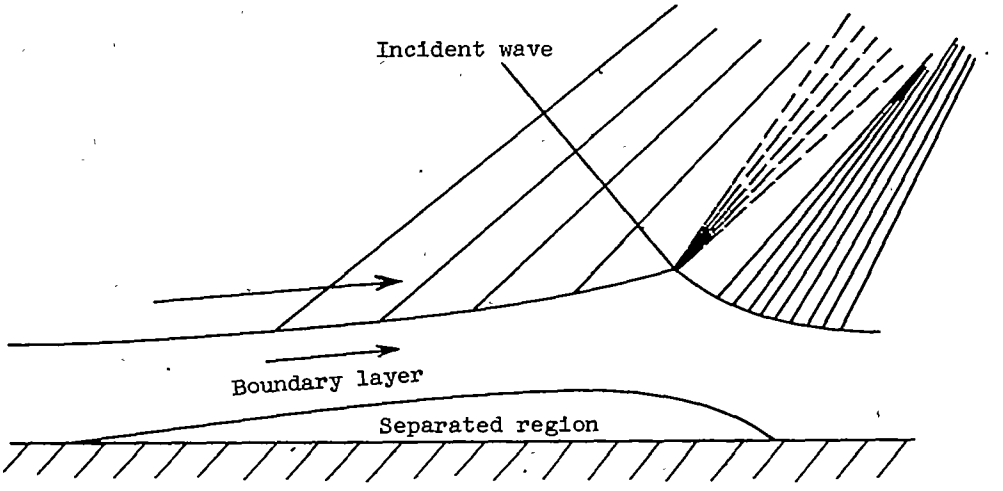

Sketch 2.

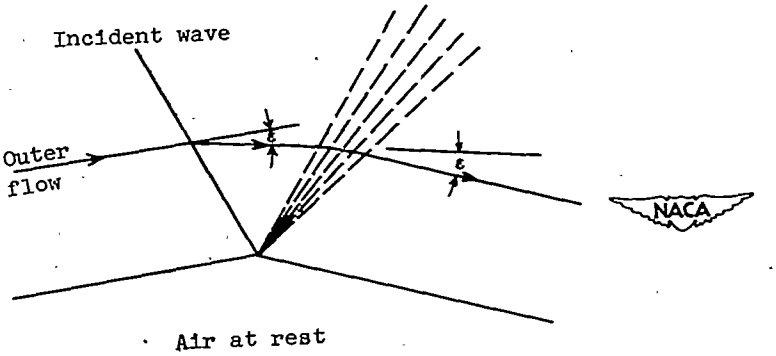

Sketch 3.

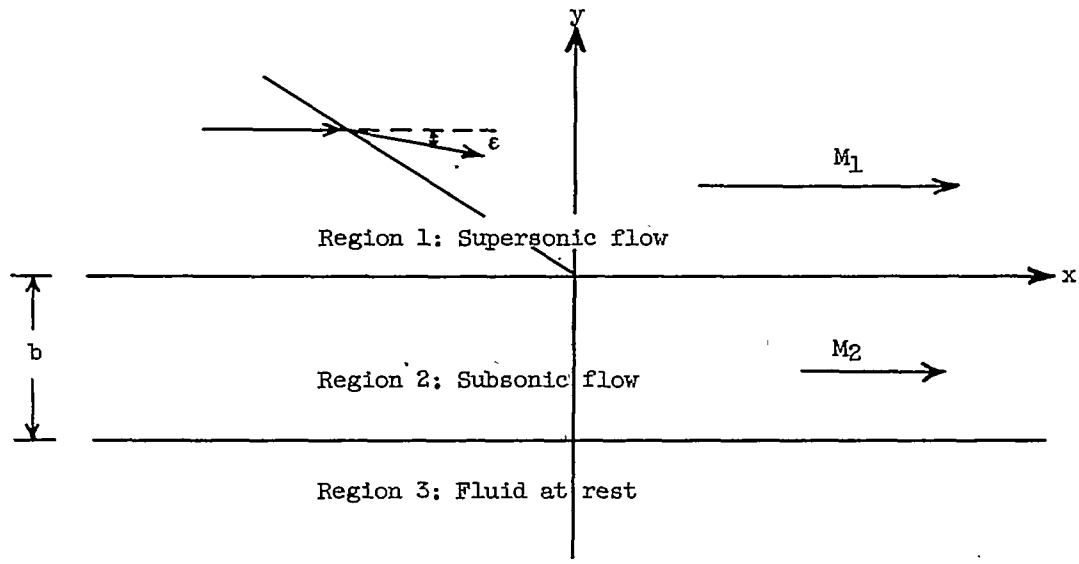

Figure 1. - Compression wave with deflection angle ε incident upon the interface between a supersonic stream and a parallel subsonic stream flowing over fluid at rest.

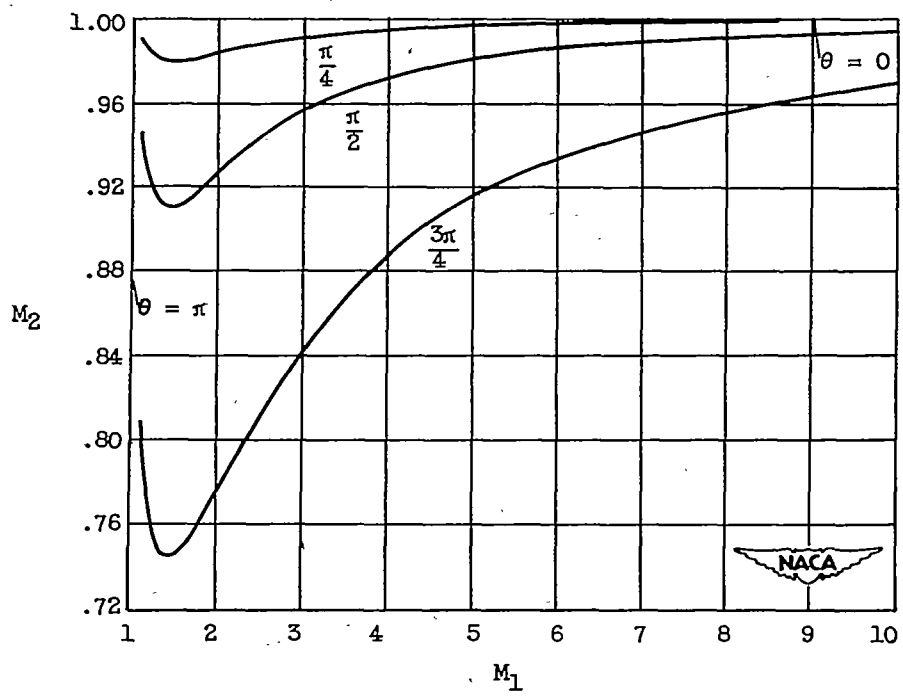

Figure 2. - Mach number M_2 in the supersonic stream against Mach number M_1 in the subsonic stream for several values of the Mach number parameter θ.

(a) Mach number parameter θ, $\pi/4$.

Figure 3. - Pressure increment Δp_U^* plotted against distance x from point of incidence of wave upon upper interface.

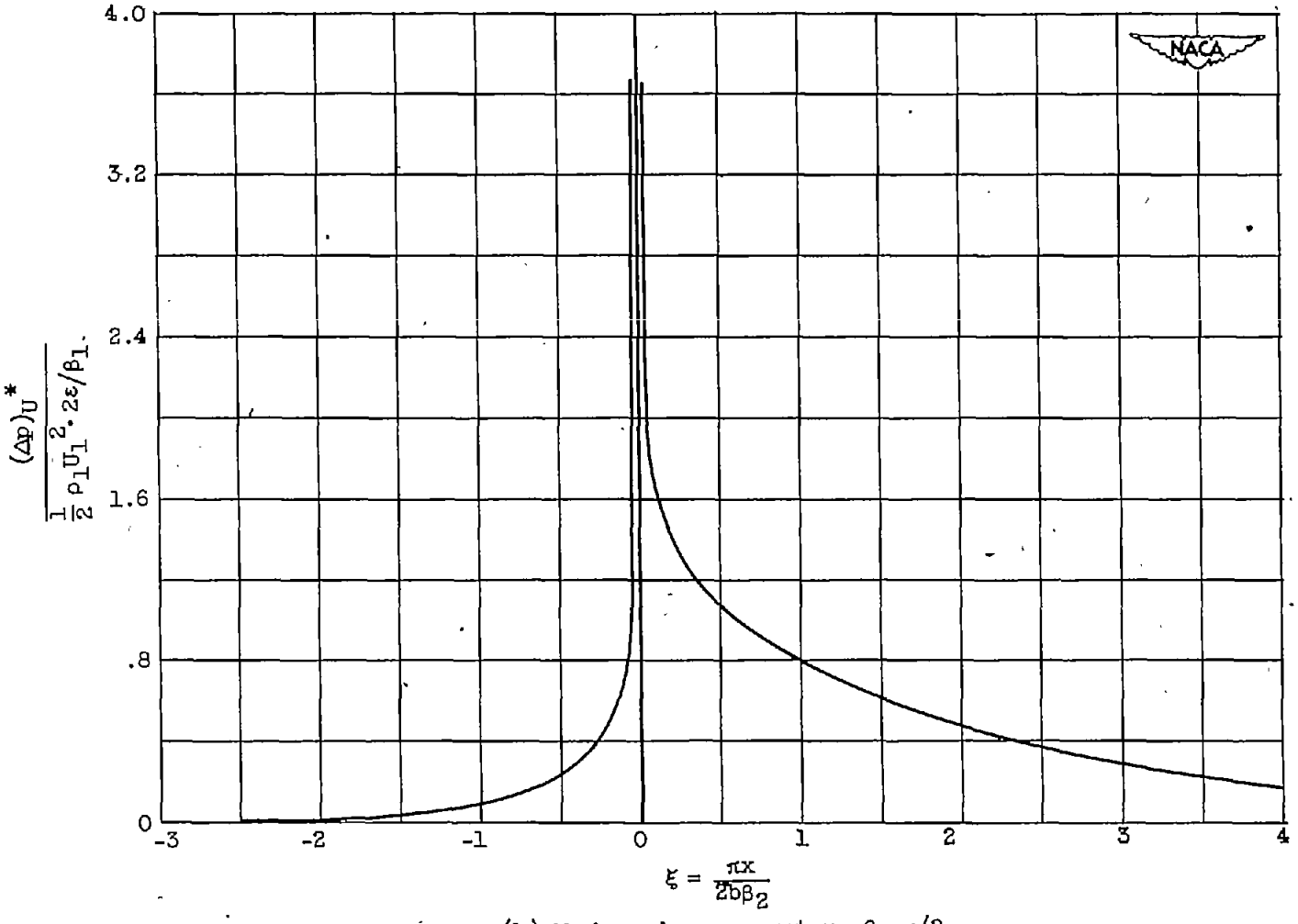

(b) Mach number parameter θ, $\pi/2$.

Figure 3. - Continued. Pressure increment Δp_U^* plotted against distance x from point of incidence of wave upon upper interface.

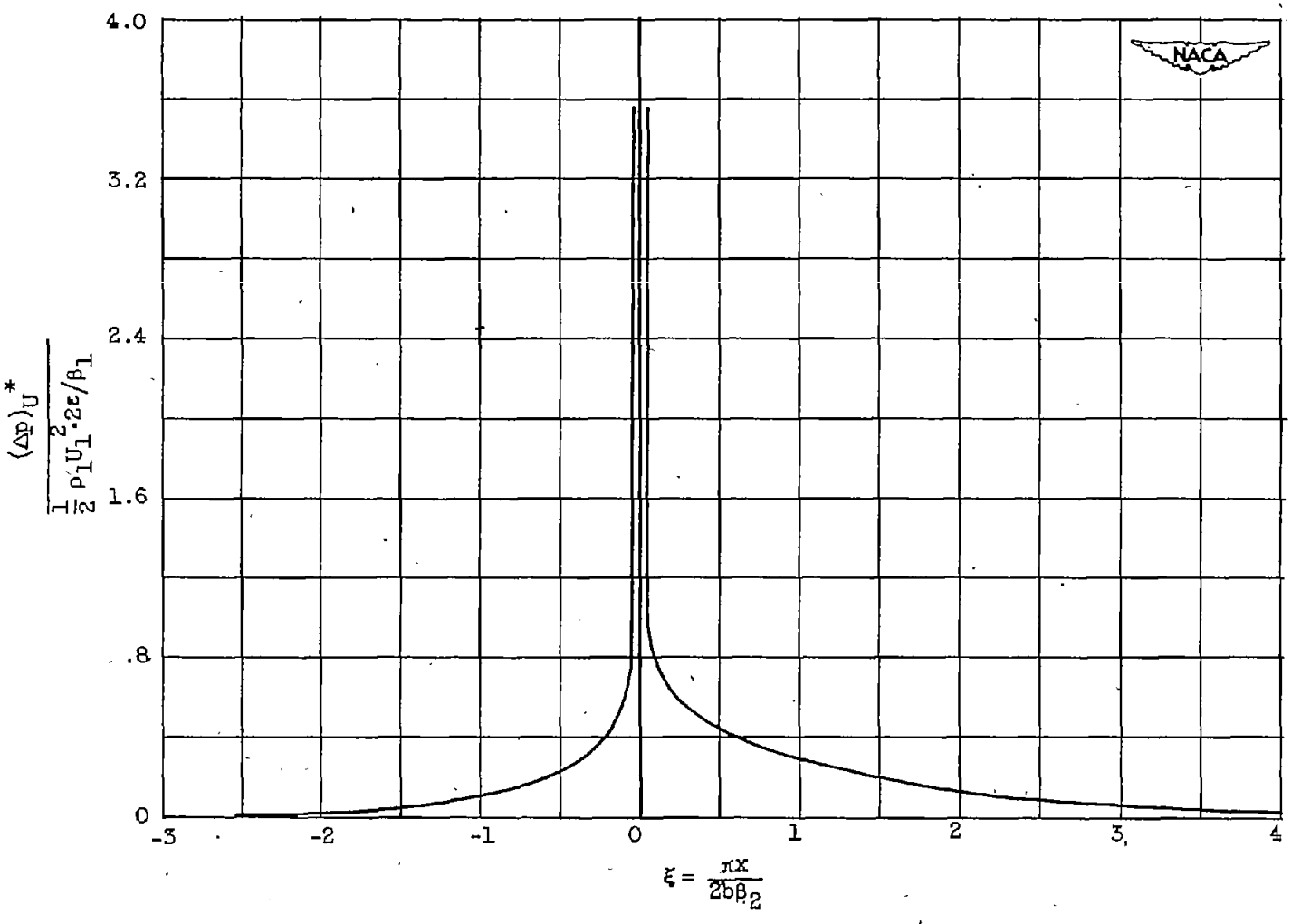

(c) Mach number parameter θ, $3\pi/4$.

Figure 3. - Concluded. Pressure increment Δp_U^* plotted against distance x from point of incidence of wave upon upper interface.

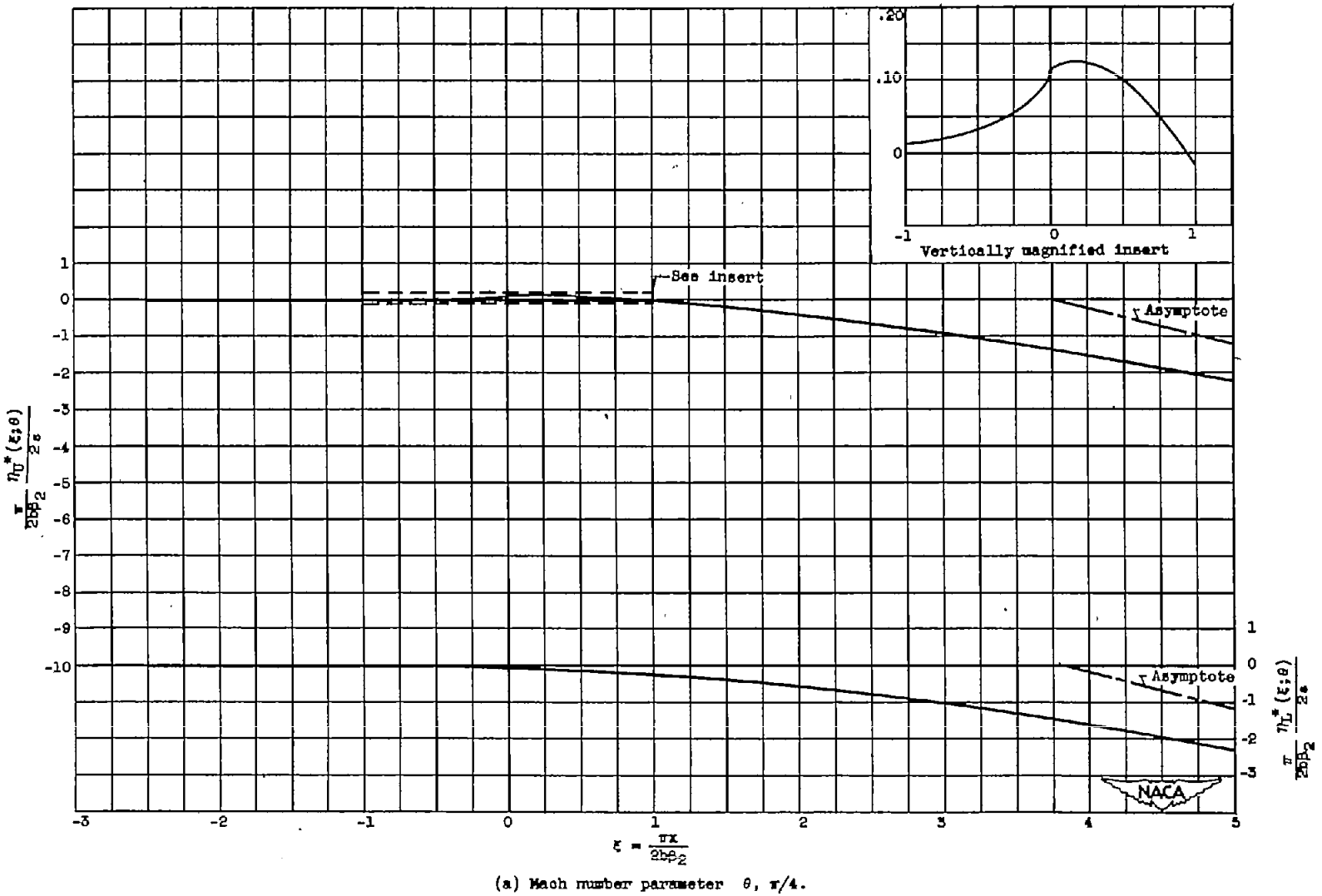

(a) Mach number parameter θ, $\pi/4$.

Figure 4. - Displacement of upper and lower interfaces plotted against distance from point of incidence of wave upon upper interface.

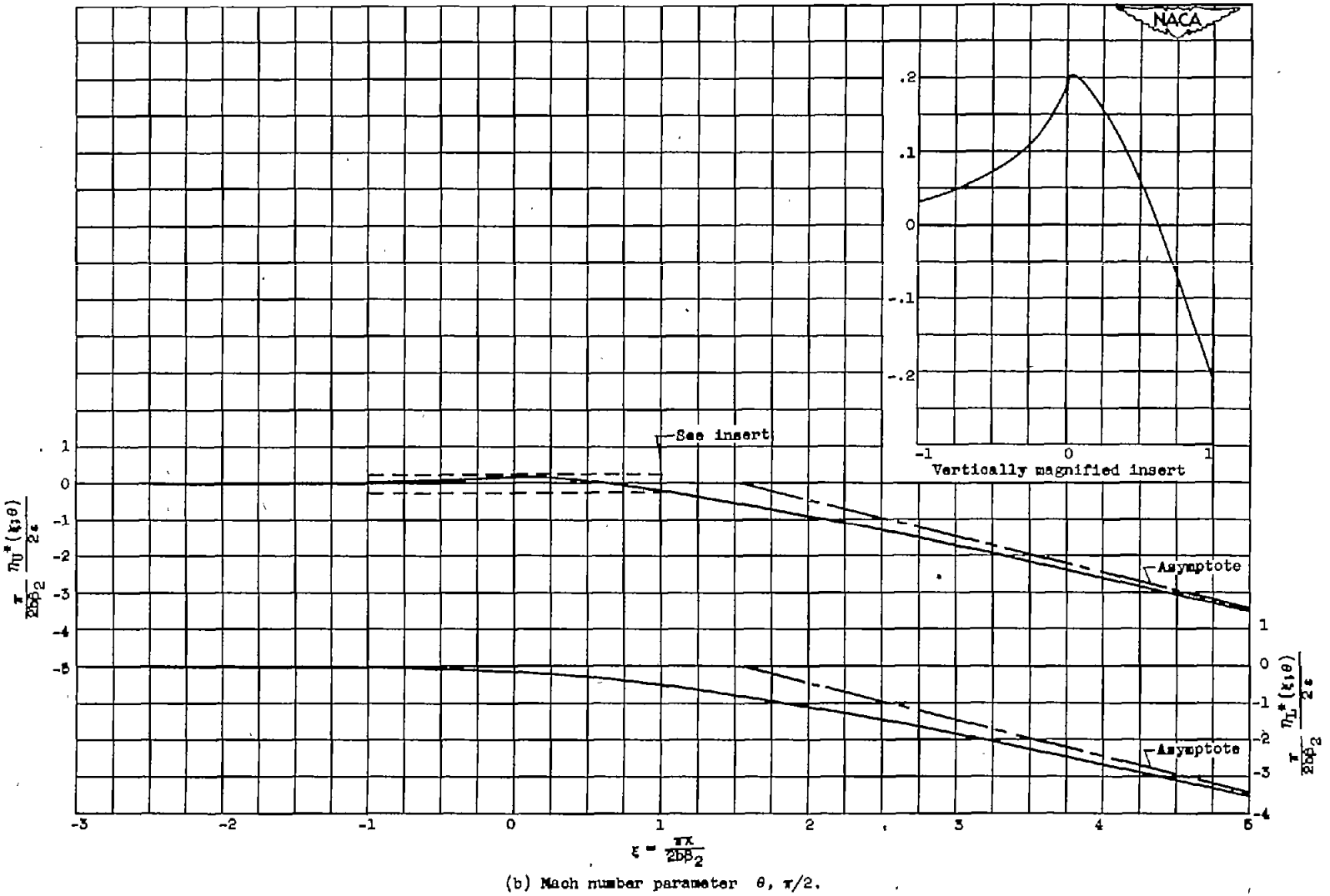

(b) Mach number parameter θ, $\pi/2$.

Figure 4. - Continued. Displacement of upper and lower interfaces plotted against distance from point of incidence of wave upon upper interface.

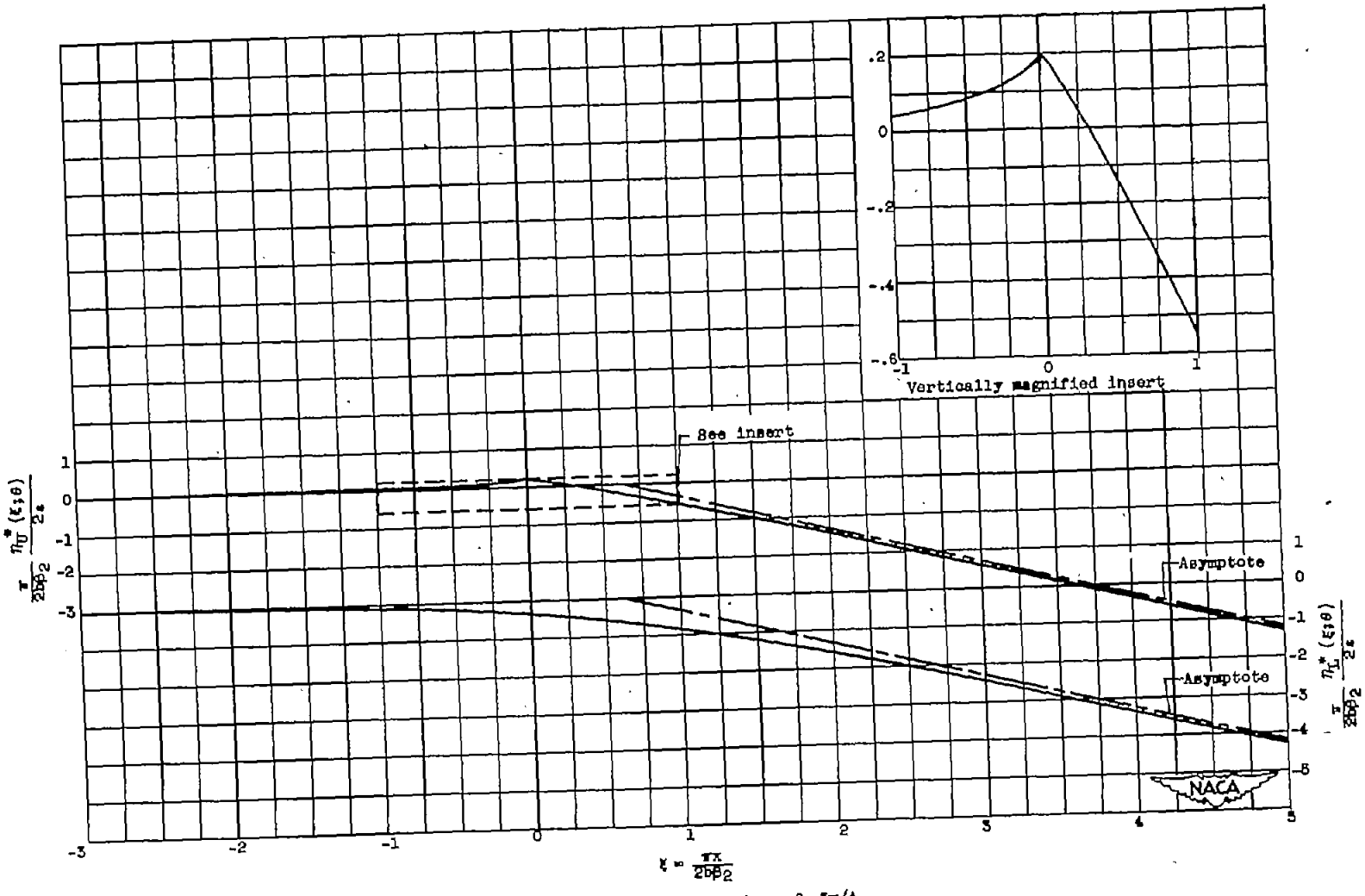

(c) Mach number parameter θ, $3\pi/4$.

Figure 4. - Concluded. Displacement of upper and lower interfaces plotted against distance from point of incidence of wave upon upper interface.

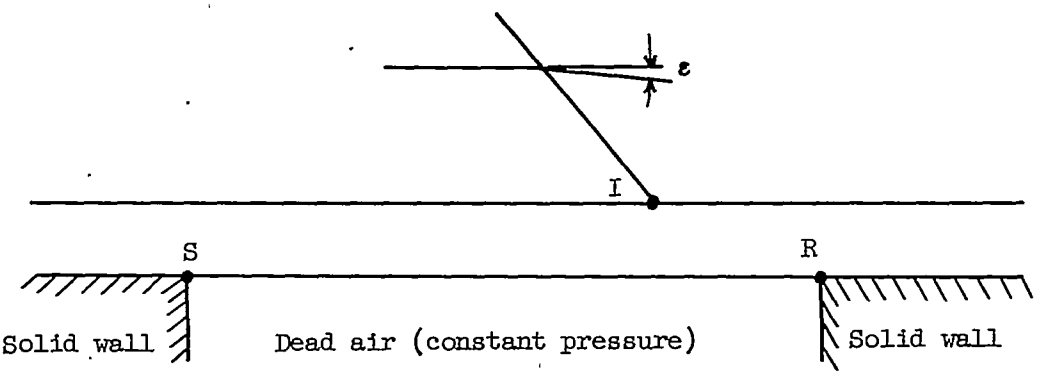

(a) Schematic.

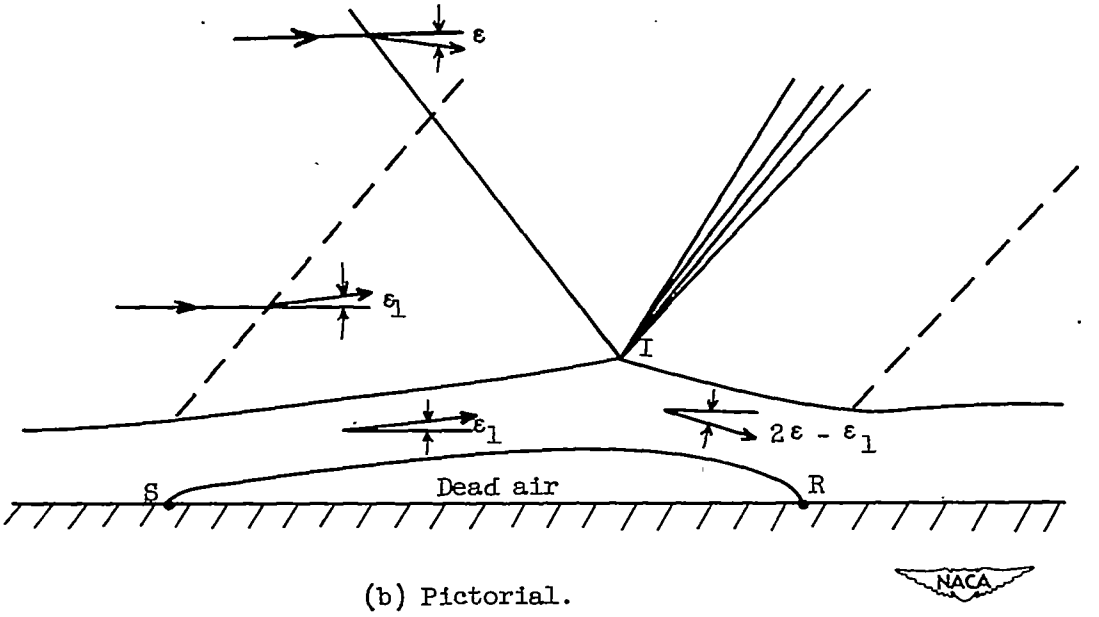

(b) Pictorial.

Figure 5. - Refinement of model of figure 1 to more closely represent shock boundary-layer interaction. (I, point of shock incidence; R, reattachment; S, initial separation.)

NACA-Langley - 12-17-52 - 1000